

AD-A135 460

MATHEMATICAL SIMULATION OF THE CARDIOPULMONARY SYSTEM
(U) TEXAS UNIV AT AUSTIN R E COLLINS ET AL. 19 AUG 83
AFOSR-TR-83-0999 AFOSR-79-0123

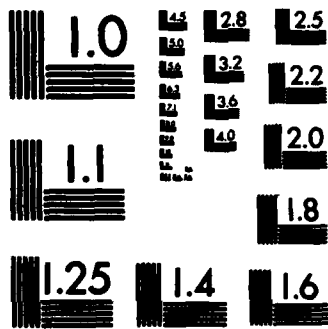
1/1

UNCLASSIFIED

F/G 12/1

NL

END
FORM
1-83
GPO



MICROCOPY RESOLUTION TEST CHART
NATIONAL BUREAU OF STANDARDS-1963-A

AFOSR-TR. 83-0999

12

FINAL REPORT

CONTRACT AFOSR 79-0123

August 19, 1983

A135460

MATHEMATICAL SIMULATION
OF THE
CARDIOPULMONARY SYSTEM

DEC 7 1983
A

R. Eugene Collins, Lee Carmack
and David Lee Martin

University of Texas at Austin
Austin, TX 78712

DTIC FILE COPY

Approved for public release;
distribution unlimited.

83 12 06 094

UNCLASSIFIED

SECURITY CLASSIFICATION OF THIS PAGE (When Data Entered)

REPORT DOCUMENTATION PAGE		READ INSTRUCTIONS BEFORE COMPLETING FORM
1. REPORT NUMBER AFOSR-TR- 88-0999	2. GOVT ACCESSION NO. A135460	3. RECIPIENT'S CATALOG NUMBER
4. TITLE (and Subtitle) Mathematical Simulation of the Cardiopulmonary System		5. TYPE OF REPORT & PERIOD COVERED Final 10/1/81-8/31/83
		6. PERFORMING ORG. REPORT NUMBER
7. AUTHOR(s) R. Eugene Collins, Lee Carmack & David Lee Martin		8. CONTRACT OR GRANT NUMBER(s) AFOSR-79-0123
9. PERFORMING ORGANIZATION NAME AND ADDRESS University of Texas at Austin Austin, Texas 78712		10. PROGRAM ELEMENT, PROJECT, TASK AREA & WORK UNIT NUMBERS 2312/A1 61102F
11. CONTROLLING OFFICE NAME AND ADDRESS Air Force Office of Scientific Research/NL Bolling AFB, DC 20332		12. REPORT DATE August 19, 1983
		13. NUMBER OF PAGES 62
14. MONITORING AGENCY NAME & ADDRESS (if different from Controlling Office)		15. SECURITY CLASS. (of this report) UNCLASSIFIED
		15a. DECLASSIFICATION/DOWNGRADING SCHEDULE
16. DISTRIBUTION STATEMENT (of this Report) Approved for public release: distribution unlimited.		
17. DISTRIBUTION STATEMENT (of the abstract entered in Block 20, if different from Report)		
18. SUPPLEMENTARY NOTES		
19. KEY WORDS (Continue on reverse side if necessary and identify by block number) Cardiopulmonary, Pulmonary, Cardiovascular, Acceleration, Ventilation, Simulation, Model		
20. ABSTRACT (Continue on reverse side if necessary and identify by block number) Multi-chamber, lumped parameter models of the pulmonary and circulatory systems have been developed which incorporate effects of whole-body accelerations (WBA) for any body orientation and a variety of breathing maneuvers. The pulmonary model has been used in an extensive study of effects of sustained WBA on pulmonary mechanics and ventilation. This study investigated the effectiveness of altering seat back angle to increase G-tolerance.		

DD FORM 1473 1 JAN 73

EDITION OF 1 NOV 65 IS OBSOLETE

UNCLASSIFIED

83 12 06 094

SECURITY CLASSIFICATION OF THIS PAGE (When Data Entered)

20. (continued)

The development and testing of the separate pulmonary and circulatory models has been reported in previous AFOSR reports, as well as the above described WBA study.

This final report describes latest efforts to incorporate feed-back and control mechanisms in the circulatory model to simulate the baroreceptor and chemoreceptor actions regulating blood flow and blood pressure in the human body. This work is not yet complete.

Also described is a partially completed study using the pulmonary model to test and implement a non-invasive technique for diagnosing ventilation distribution dysfunctions.

This technical report has been reviewed and approved for public release IAW AFR 190-12. Distribution is unlimited.

MATTHEW J. KERPER

FINAL REPORT Chief, Technical Information Division
AFOSR - 79-0123
August 1983

MATHEMATICAL SIMULATION OF
THE CARDIOPULMONARY SYSTEM



R. Eugene Collins (Principal Investigator),
Lee Carmack and David Lee Martin

University of Texas at Austin, Austin, TX 78712

SEARCHED	INDEXED
SERIALIZED	FILED
AUG 25 1983	
AFOSR	
Special	

Al

ABSTRACT

Multi-chamber, lumped parameter models of the pulmonary and circulatory systems have been developed which incorporate effects of whole-body accelerations (WBA) for any body orientation and a variety of breathing maneuvers. The pulmonary model has been used in an extensive study of effects of sustained WBA on pulmonary mechanics and ventilation. This study investigated the effectiveness of altering seat back angle to increase G-tolerance.

The development and testing of the separate pulmonary and circulatory models has been reported in previous AFOSR reports, as well as the above described WBA study.

This final report describes latest efforts to incorporate feedback and control mechanisms in the circulatory model to simulate the baroreceptor and chemoreceptor actions regulating blood flow and blood pressure in the human body. This work is not yet complete.

Also described is a partially completed study using the pulmonary model to test and implement a non-invasive technique for diagnosing ventilation distribution dysfunctions.

a

PART I

FEEDBACK AND CONTROL IN THE CARDIOPULMONARY SIMULATOR

INTRODUCTION

A computer simulator of the human cardio-pulmonary system has been developed as two distinct models. The first model is a pulmonary simulator which has proved to be a valuable stand-alone system for the evaluation of pulmonary mechanics and ventilation during whole body acceleration (WBA). This pulmonary simulator has been described in detail in previous reports and a working copy has been sent to Wright-Patterson AFB. The second model is a circulatory simulator which has also been described in detail in previous reports.

The achievements during this report period are 1) modification of the circulatory model to increase its controllability, 2) the inclusion of feedback mechanisms to the circulatory system, and 3) interfacing the pulmonary and circulatory models to work in conjunction with each other as a single simulator.

A comprehensive numerical model of the feedback and control systems which regulate the cardiovascular system was devised and incorporated into the digital computer simulator of the cardiovascular and pulmonary systems. The model is designed specifically to study the effects of short term whole-body acceleration on the cardiovascular system as encountered by astronauts and pilots of high performance aircraft. The feedback systems include the sympathetic and parasympathetic neural control of the cardiovascular system, resulting from feedback loop responses. These feedback loop responses are due to 1) arterial pressure changes acting upon specialized sensors, i.e. baroreceptors, and 2) changes in blood gas concentrations acting upon

chemoreceptors. The controlling mechanisms include variations of heart rate, contractility, and the peripheral resistances and compliances in the vascular system.

The completed cardio-pulmonary computer simulator is a multi-chambered model representing the human cardiovascular and pulmonary systems, including pulsatile blood flow and gas transport and exchange. It represents an active, time varying, nonlinear model with non-linear elastic characteristics, pressure dependent flow resistances, and arterial pressure and blood gas concentration feedback systems.

BACKGROUND

Many models have been developed to represent the pulmonary or cardiovascular systems; however, none address the same functional parameters or level of complexity as the current model. Some models are limited to specific anatomical features, such as heart, systemic arterial vasculature, or venous vasculature. Other models are designed to study different functions, such as fluid balance, long term regulation, or metabolism. Few models include the complexity of multi-elements, nonlinear relationships, or dependent elements. Of the models including gravitational effects on the cardiovascular system, none have been as complete as the current model.

Detailed descriptions of the pulmonary model and the cardiovascular model have been reported previously. This report will review some of these details to facilitate describing the inclusion into the circulatory model of feedback and controllability systems.

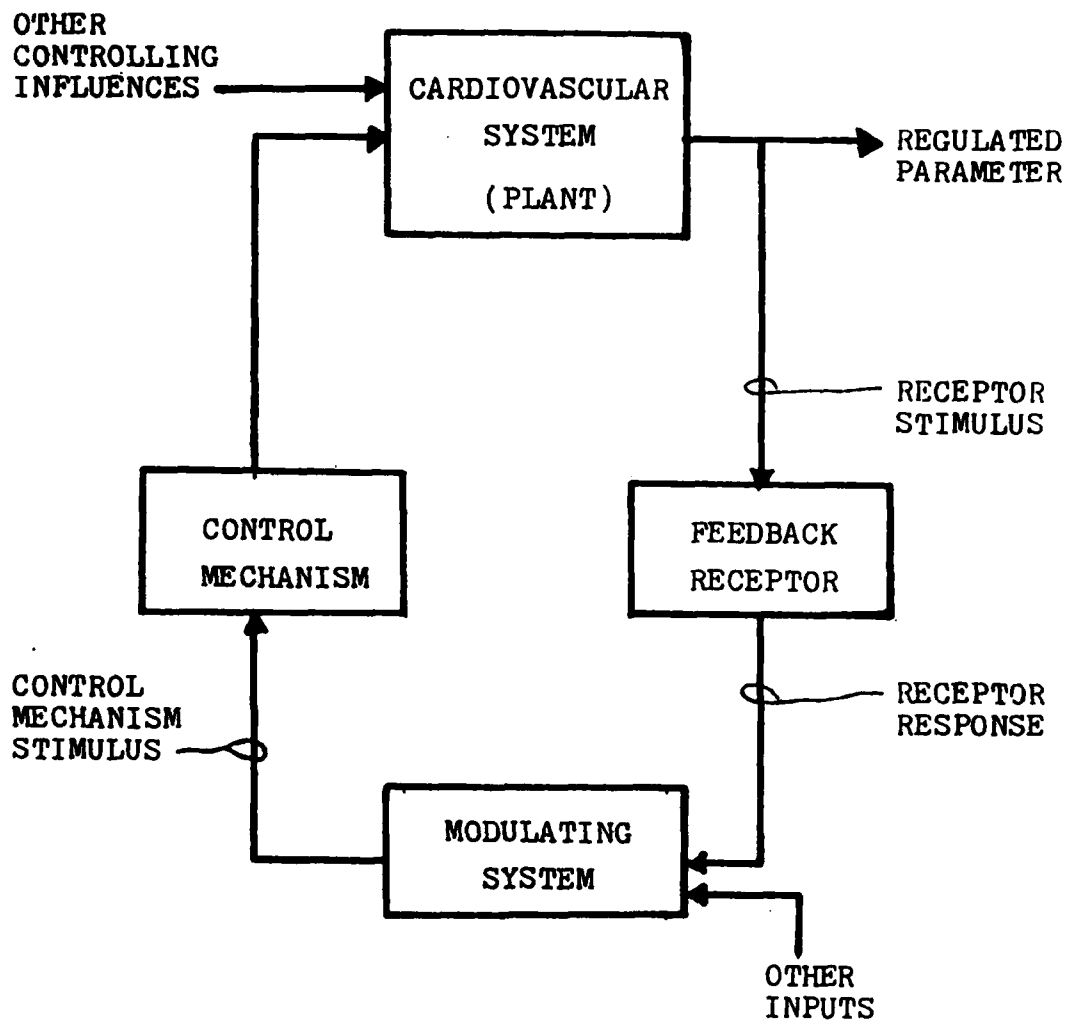
PHYSIOLOGICAL BACKGROUND

A cardiovascular feedback system can be modeled as a controlled system (plant), a feedback loop, and a controlling mechanism. The controlled system represents that portion of the cardiovascular system to be regulated. The feedback loop portion consists of a receptor stimulus (a parameter from the controlled system), feedback receptors, receptor response, any modulating effects, and the resultant stimulus to activate the control mechanism. The control mechanisms are the physiological parameters which are altered, due to the control mechanism stimuli, resulting in the regulation of the controlled system. Figure 1 shows a block diagram of a feedback system.

There are many cardiovascular feedback systems. However, in limiting the model to the study of short term effects due to whole body acceleration, two feedback systems exhibit the predominant effects. They are the baroreceptor reflex and the chemoreceptor reflex (see Figure 2).

The baroreceptor reflex is particularly critical in regulating gravitational or orientational changes. This feedback system is stimulated by arterial pressure and results in controlling: 1) heart rate, 2) cardiac contractility, and 3) vascular resistance and compliance.

The arterial pressure in the carotid sinus and aortic arch is the stimulus acting on the pressoreceptors (baroreceptors) located in the same areas. The efferent nerve response from the baroreceptors decreases in relation to a carotid pressure decrease (Warner, 1958). This receptor response then enters the central nervous system, CNS, where it is modulated with other CNS stimuli, resulting in new



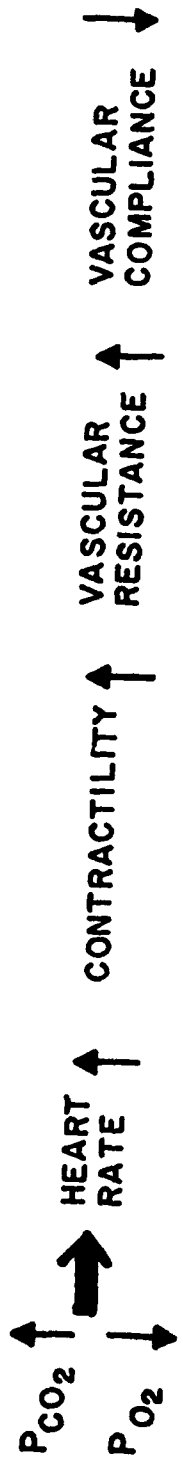
FEEDBACK SYSTEM BLOCK DIAGRAM

Figure 1

BARORECEPTOR REFLEX



CHEMORECEPTOR REFLEX



CARDIOVASCULAR FEEDBACK SYSTEMS

Figure 2

efferent neural signals to the controlling mechanisms. For these efferent neural signals, the sympathetic frequency of stimulation to the controlling mechanism is increased while the parasympathetic frequency of stimulation is decreased. The relationship describing the CNS input/output and modulation with other efferent signals is not clearly understood. However, relations between carotid pressure and sympathetic firing (Kezdi and Geller, 1968) and carotid pressure and vagal firing (Katona and Barnett, 1970) have been made.

The responses of the three controlling mechanisms due to the efferent neural signals complete the description of this feedback system. The heart rate increases in response to increased sympathetic activity and decreased parasympathetic activity (Warner and Cox, 1962). The two neural paths have different time delays before their effects are seen. The sympathetic response can be delayed 20 seconds while the parasympathetic response is immediate (Wang and Borison, 1947). The carotid pressure change has been related to the heart rate by Scher and Young (1970) and Glick and Braunwald (1965).

The second controlling mechanism is heart contractility, or force of contraction, that is not due to the Frank-Starling effect of stretch. The contractility will increase with increased sympathetic activity and decreased parasympathetic activity (Levy, 1963 and Rushmer, 1962). Additionally, the contractility will vary due solely to changes in heart rate (Koch-Weser and Blinks, 1963).

The third controlling mechanism of the baroreceptor reflex feedback system is vascular compliance, which is proportional to vascular resistance. The vascular compliance decreases resulting in an increased vascular resistance when sympathetic activity to vascular

tissue increases and parasympathetic activity decreases. Not all vascular compliances change similarly. The coronary arteries and cerebral vessels do not constrict when the rest of the vasculature does (Gregg and Fischer, 1963, and Rapela and Green, 1964).

Another important type of feedback system is the chemoreceptor reflex. It is stimulated by the blood gases and results in controlling: 1) heart rate, 2) contractility, 3) vascular resistance, and 4) respiration. This blood gas feedback system can be divided into two loops. In the first, blood gases in the aortic arch and carotid sinus are the stimuli of chemoreceptors located in the aortic bodies and carotid bodies. A decrease in O_2 , an increase in CO_2 , or decrease in pH will cause the efferent nerve activity from the chemoreceptors to the CNS to increase. As with the baroreceptors, the CNS modulates this receptor response with other CNS stimuli. With the above gas changes, the efferent neural signals from the CNS to the controlling mechanisms are altered such that the sympathetic frequency of stimulation is increased while the parasympathetic frequency of stimulation is decreased (Von Euler, et al., 1939).

The second feedback loop of this blood gas feedback system has its chemoreceptors located in the medulla. Similar to the loop described above, an increase in CO_2 , or decrease in O_2 or pH will cause the CNS to alter the frequency of efferent neural signals to the controlling mechanisms. The sympathetic stimuli increase in frequency while the parasympathetic decrease.

Although these two loops are activated by the same stimuli, i.e., blood gas concentration, they are not equally as sensitive to the individual gases. Similarly, even though these two loops both affect

the same controlling mechanisms (heart rate, contractility, vascular resistance, respiration rate, and tidal volume), the degree to which each loop affects these control mechanisms is different.

Basically, the effect on these control mechanisms is the same as described for the baroreceptors. With an increase in frequency of sympathetic activity, and a decrease in frequency of parasympathetic activity, heart rate, contractility, and peripheral resistance all increase. In addition, these loops affect the respiration. With a similar change in sympathetic and parasympathetic activity, the respiration rate and the tidal volume increase.

Many additional feedback systems exist in the circulatory system, including autoregulation and the ischemic reflex. However, the two described above exhibit the predominant effects in the types of situations to be modeled.

MODEL DESCRIPTION

In order to understand how these feedback systems are modeled, it is necessary to first describe the cardiovascular model into which they are incorporated. The cardiovascular system is represented by a twenty-four chamber model including a four chamber heart (see Figure 3). The chambers represent various portions of the cardiovascular system, including the arterial vascular network, several capillary beds, several venous vascular networks, and the four chambers of the heart.

The mechanics of blood circulation for a generalized chamber element can be described using three equations. The first treats the

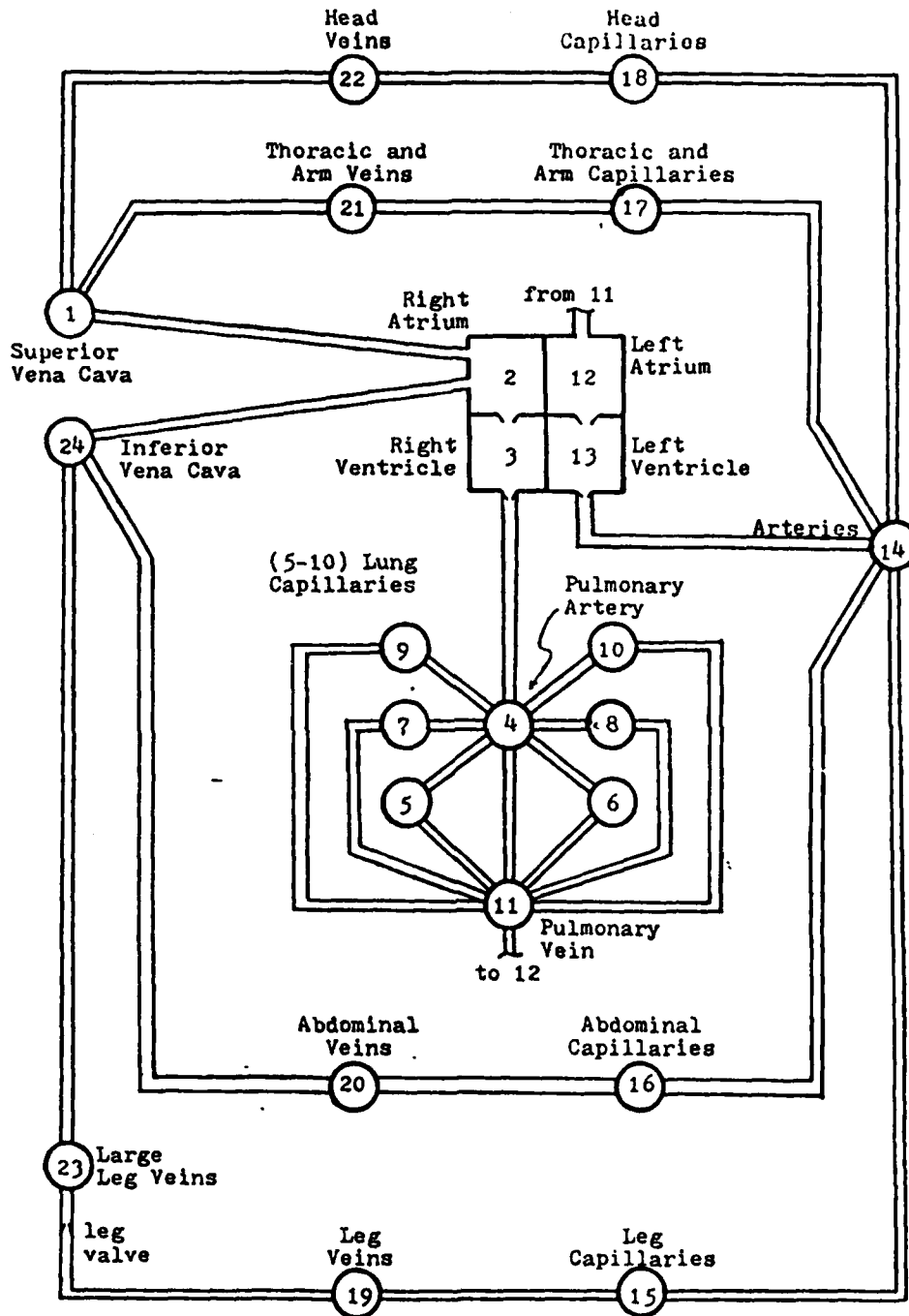


DIAGRAM of the CARDIOVASCULAR MODEL

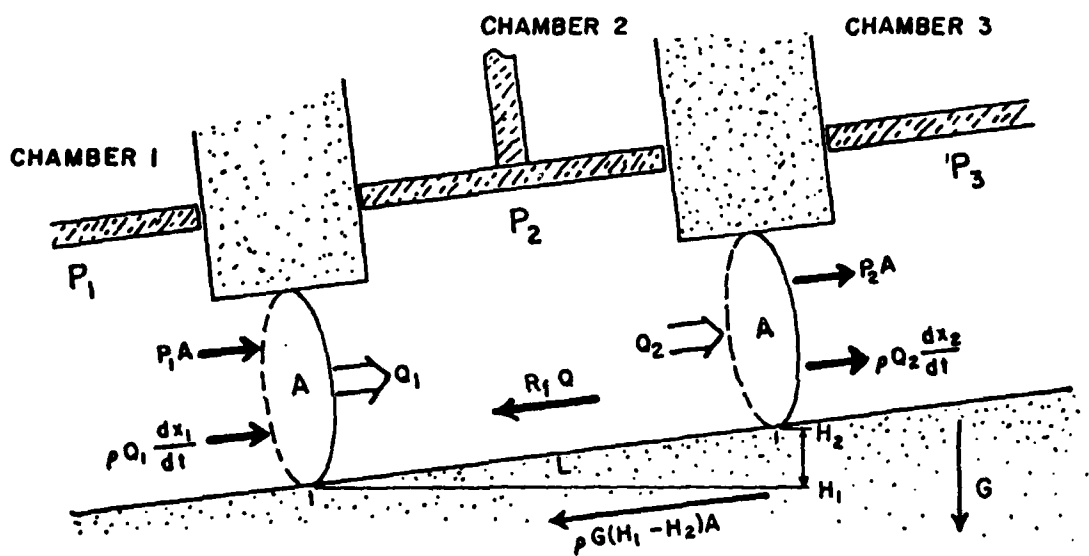
Figure 3

axial motion of the blood through the blood vessels. The second treats the transverse motion of the blood, vessel wall, and surrounding tissue, and the third assumes conservation of mass for the blood in the chambers.

Axial Motion

The equations for axial motion of the blood through a circulatory element are based on the conservation of momentum written in terms of forces as source terms (see Figure 4). The rate of change in axial momentum of blood in the vessel, $\frac{d(\rho Lq)}{dt}$, can be described in terms of the density of blood, ρ , the vessel length, L , and the mean volumetric flow rate through the vessel, q . According to Newton's second law of motion, this change in momentum is equal to the algebraic sum of the axial forces acting on the blood in the vessel. The forces acting consist of the pressure force of the fluid at the inlet, $P_1 A_1$, and the outlet, $-P_2 A_2$, the force of gravity, $\rho g(h_1 - h_2)A$, the inertial force of the blood at the inlet, $\rho q_1 \frac{dx_1}{dt}$, and at the outlet, $-\rho q_2 \frac{dx_2}{dt}$, and the viscous drag force at the vessel walls, fA_s . Here, A_s is the total surface area of the vessel; A is the average cross sectional area of the vessel; $(h_1 - h_2)$ is the distance separating the inlet and outlet ends of the vessel along the direction of the gravitational acceleration, g ; q_1 and q_2 are inlet and outlet volumetric flow rates, $\frac{dx_1}{dt}$ and $\frac{dx_2}{dt}$ are the inlet and outlet velocities; and f is the total drag force per unit area of vessel wall. Assuming a uniform cross sectional area, i.e., $A_1 = A_2 = A$, and assuming fA_s can be approximated by a resistance \bar{R}_f times the mean volumetric flow rate, q , the equation can be written as:

CHAMBER FLOW DYNAMICS

AXIAL MOTION

$$\frac{d(\rho L Q)}{dt} = \rho Q_1 \frac{dx_1}{dt} - \rho Q_2 \frac{dx_2}{dt} + P_1 A - P_2 A + \rho G (H_1 - H_2) A - R_f Q$$

Figure 4

$$\frac{d(\rho Lq)}{dt} = \rho q_1 \frac{dx_1}{dt} - \rho q_2 \frac{dx_2}{dt} + P_1 A - P_2 A + \rho g(h_1 - h_2)A - \bar{R}_f q \quad (1a)$$

This can be rearranged to get:

$$\frac{\rho L}{A} \frac{dq}{dt} = \rho \frac{dx_1}{dt} - \rho \frac{dx_2}{dt} + P_1 - P_2 + \rho g(h_1 - h_2) - R_f q \quad (1b)$$

where $R_f = \bar{R}_f/A$ and R_f is a function of volume.

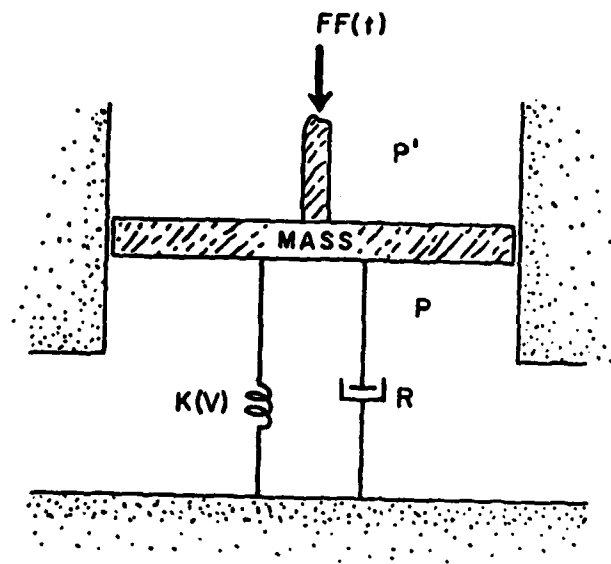
Transverse Motion

The equations for transverse motion of the vessel wall and surrounding tissue are also derived from Newton's second law (see Figure 5). The sum of the forces acting on the vessel wall and surrounding tissue are equal to the mass of the wall and tissue, m , times its acceleration, a . In terms of volume of the chamber element, V , the term ma can be expressed as $\frac{m}{A} \frac{d^2 V}{dt^2}$, where A is the surface area.

The forces acting on the vessel wall consist of the force due to blood pressure in the vessel, PA ; the force due to external pressure on the vessel and surrounding tissues, AP' , the force due to the elastance pressure from the muscular tissue surrounding the vessel, $-K(V)(V-V_{eq})$; the force due to the friction of the wall on surrounding tissues, $-R \frac{dV}{dt}$, and in the case of the heart chambers, an external force due to heart contraction, $FF(t)$. This gives the equation:

$$\frac{m}{A} \frac{d^2 V}{dt^2} = AP - AP' - K(V)(V-V_{eq}) - R \frac{dV}{dt} - FF(t) \quad (2)$$

CHAMBER WALL DYNAMICS



TRANSVERSE MOTION

$$\frac{M}{A_s} \frac{d^2V}{dt^2} = A_s P - A_s P' - K(V)(V - V_{eq}) - R \frac{dV}{dt} - FF(t)$$

Figure 5

Here $K(V)$ is a nonlinear compliance term dependent on volume; R is a resistance term associated with frictional resistance of tissue; and $FF(t)$ is a time varying function representing the force due to contraction of the heart.

Conservation of Mass

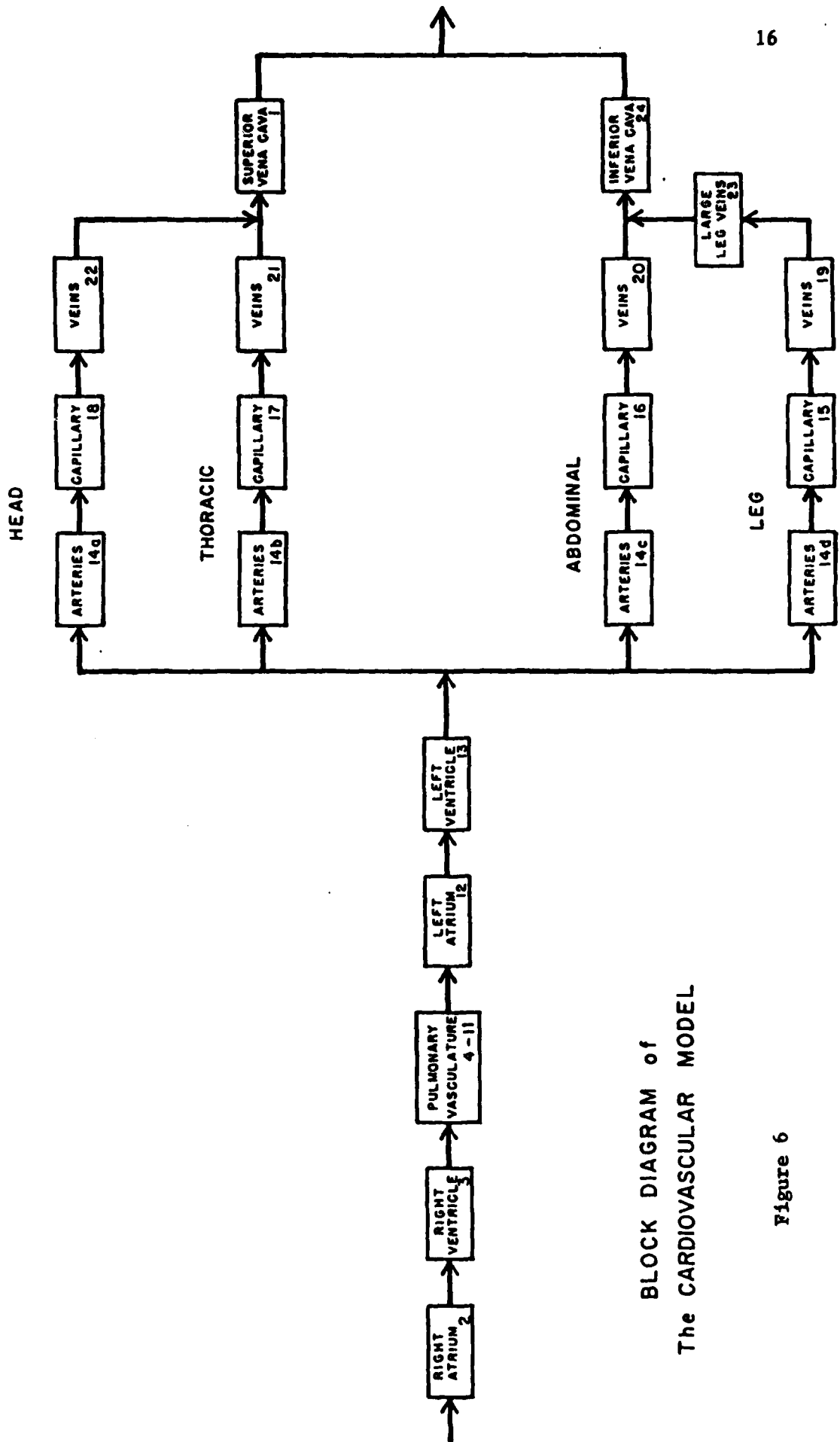
Based on conservation of mass, the rate of change in volume of a chamber, $\frac{dV}{dt}$, must equal the difference between the sum of the volumetric flows into the chamber, q_{in} , and the sum of the volumetric flows out of the chamber, q_{out} . This gives the equation:

$$\frac{dV}{dt} = \sum q_{in} - \sum q_{out} \quad (3)$$

The above equations represent a generalized chamber in the twenty-four chamber cardiovascular model. However, each individual chamber can be simplified according to the particular dynamics of that chamber. For example, only the four heart chambers have the forcing function term $FF(t)$ representing an external force due to heart contraction.

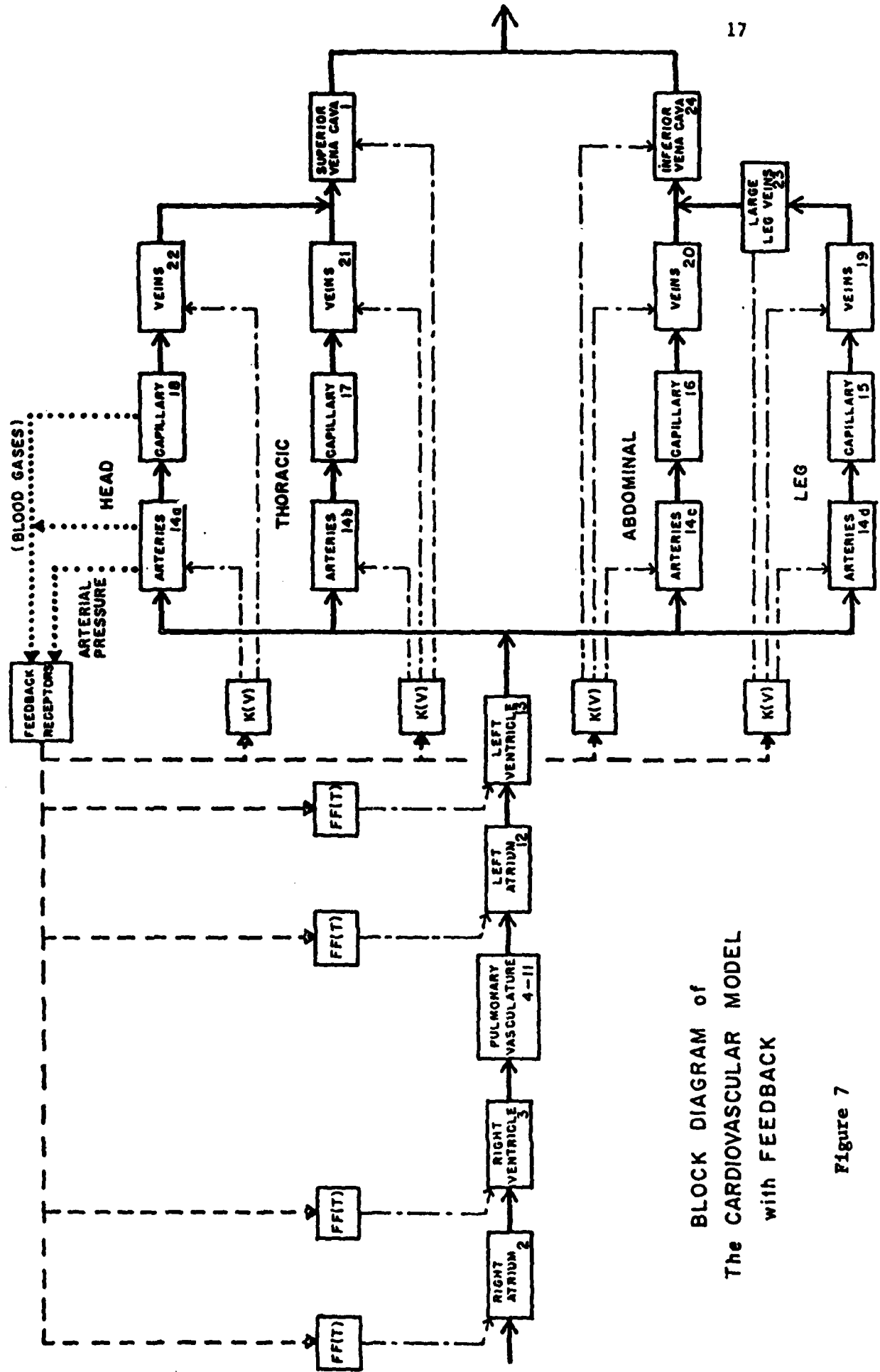
The family of equations describing the cardiovascular system can be illustrated as a simple block diagram with each block representing a particular portion of the system (see Figure 6). From such a block diagram, it can be clearly illustrated where the feedback systems will be included (see Figure 7). The dotted lines represent stimuli to the feedback receptors. The blocks labeled $FF(t)$ represent the feedback responses changing the forcing function to alter heart rate and contractility. The blocks labeled $K(V)$ represent the feedback

responses altering the vascular compliance term which changes the vascular resistance.



BLOCK DIAGRAM of
The CARDIOVASCULAR MODEL

Figure 6



BLOCK DIAGRAM of
The CARDIOVASCULAR MODEL
with FEEDBACK

Figure 7

MODEL DESCRIPTION OF CONTROL AND FEEDBACK SYSTEMS

The physiological feedback reflexes described earlier sense three parameters. The carotid blood pressure is sensed by the baroreceptor reflex and the partial pressure of carbon dioxide, P_{CO_2} , and the partial pressure of oxygen, P_{O_2} , are sensed by the chemoreceptors. Both of these reflexes result in controlling heart rate, heart contractility, and vascular compliance which affects the vascular resistance (see Figure 8).

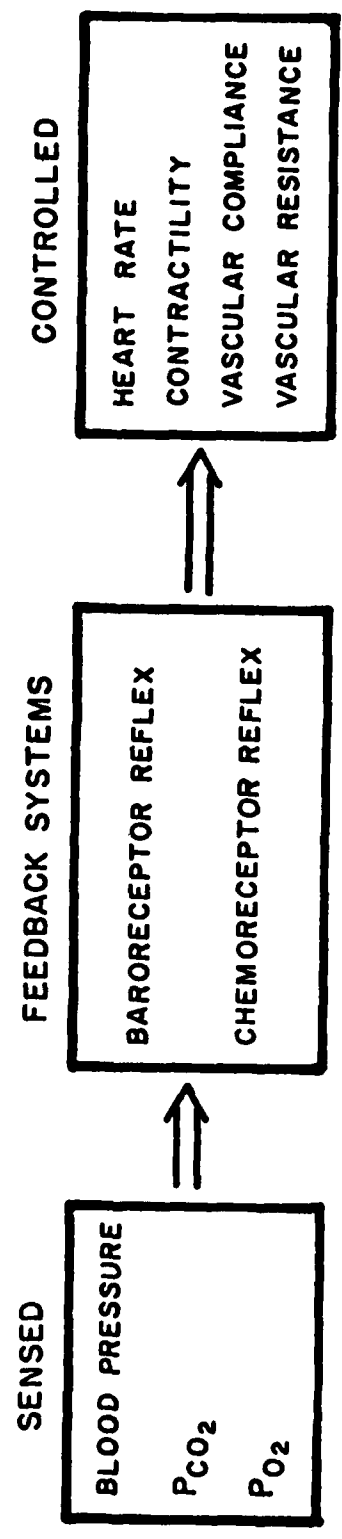
The model can simulate these changes by varying just two parameters. First, the model variable for the forcing function, $FF(t)$, of each heart chamber can be altered to control the heart rate and contractility of the heart. Second, the vascular compliance term, $K(V)$, of each chamber can be altered to control vascular compliance which will result in a change in vascular resistance.

To model the physiological reflexes, both the forcing function terms and the chamber vascular compliance terms should be appropriately varied in response to changes in either carotid blood pressure or the partial pressure of CO_2 or the partial pressure of O_2 (see Figure 7).

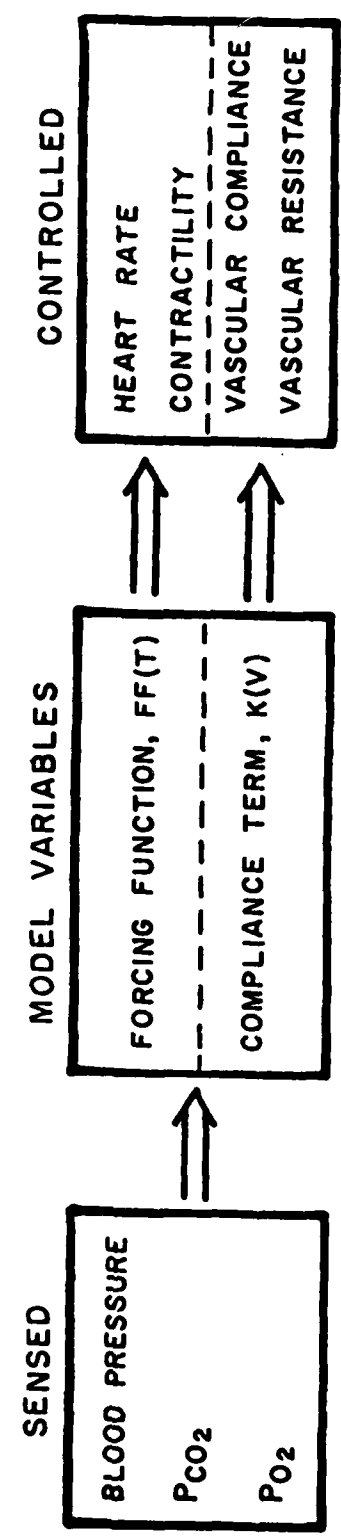
To simulate a four chamber pulsating heart with variable heart rate and variable contractility, a new heart model was developed which included a new forcing function. The forcing function, $FF(t)$, as shown in Equation 2, is a time varying function representing the force and duration of a contraction of the heart. For each different heart rate and contractility, a unique forcing function is required.

The duration of ventricular contraction closely corresponds to the Q-T interval, QT_{int} , in an electrocardiogram. An equation

PHYSIOLOGICAL REFLEXES



MODEL SIMULATION



CARDIOVASCULAR FEEDBACK and CONTROL

Figure 8

relating heart rate, HR, to ventricular contraction time was developed using data on Q-T intervals (Ashman, 1956).

Since the heart rate is inversely proportional to its pulse interval, RR_{int} , we can write the equation for the ventricles as:

$$\frac{1}{QT_{int}} = 1.6 + \frac{1}{RR_{int}} \quad (4)$$

where $HR = 60 \times RR_{int}$.

Similar data does not exist for the duration of atrial contraction, PR_{int} , but using known values at several heart rates and assuming a slope similar to that for the ventricles, the following equation was derived:

$$\frac{1}{PR_{int}} = 5.4 + \frac{1}{RR_{int}} \quad (5)$$

Now, for a given heart rate the appropriate forcing function, FF, for each heart chamber can be computed.

$$FF = PSAMP \cdot \exp \left\{ - \left[\frac{\text{Alpha} \cdot |t - \text{PSCENT}|^4}{1 - \left| \frac{t - \text{PSCENT}}{\text{PSEND} - \text{PSCENT}} \right|^4} \right] \right\} + PPAVE \quad (6)$$

where: $t = \text{time}$

$\text{PSEND} = \text{time at the end of FF, or time at start of contraction} + \text{the duration of the contraction}$

$\text{PSCENT} = \text{time midway into FF}$

$\text{Alpha} = \text{a constant controlling the shape of the curve}$

$\text{PSAMP} = \text{variable controlling the amplitude of the FF}$

PPAVE = addition force on chamber due to plural cavity pressure.

Changing variable PSAMP corresponds to changing the contractility of the heart chambers.

Physiologically, contractility or inotropic effect cannot be measured directly; however, a good indication of contractility is the maximum rate of change in the pressure, $\frac{dP}{dt}$ Max, (Guyton, 1971). By infusion of isoprenaline, which increases contractility, and by controlling the heart rate, a linear relationship can be seen between increase in heart rate and $\frac{dP}{dt}$ Max (Furnival, et al., 1970). This relationship was used initially to modify PSAMP to generate a $\frac{dP}{dt}$ Max at a given heart rate. However, it was modified by making repeated computer runs so that stroke volumes and cardiac outputs would correspond to known values under various degrees of sympathetic and parasympathetic stimulation (Guyton, 1971). Therefore, for a desired heart rate, using equations 4 and 5, the duration of the forcing functions and heart rate intervals can be calculated for the four heart chambers, and the degree of contractility for each can be set by calculating the values of PSAMP. Selection of the appropriate vascular compliance will be discussed later.

Physiologically, regardless of the type of receptor stimulus used as input to the feedback loop (blood pressure, P_{CO_2} or P_{O_2}) the output to the controlling mechanism will always be in terms of sympathetic and parasympathetic neural activity. Also, regardless of the type of controlling mechanism (heart rate, contractility, or vascular compliance), the input stimulus will always be expressed in terms of sympathetic and parasympathetic neural activity.

This relationship implies that if the resultant sympathetic and parasympathetic stimulus due to combined stimulation by carotid blood pressure, P_{CO_2} , and P_{O_2} , could be found, then the controlling mechanisms could each be calculated from that. Much data exists comparing sympathetic and parasympathetic activity to heart rate and other functions. Also, there are many investigations concerning activation of receptor sites and the resulting neural responses. However, sufficient data does not yet exist to bring these systems, from receptor to controlling mechanism, into a unified theory based on sympathetic and parasympathetic activity. A primary problem is a lack of quantitative information on interactions in the central nervous system.

The approach used in this model was to take a lumped systems approach by looking at the receptors stimulus (carotid blood pressure) and a controlling mechanism output (heart rate). Initially, the mean carotid pressure, P_c , at the baroreceptors is calculated for the current heartbeat. The carotid pressure is calculated as the arterial chamber pressure plus the hydrostatic pressure between the heart and the carotid artery where the baroreceptors are located. This pressure is compared to a set normal functioning carotid pressure, P_{cj} . The difference in carotid pressure, ΔP_c , is used to compute the change in heart rate necessary to return the carotid pressure to its normal value. The change in heart rate, ΔHR , is the difference between the normal operating heart rate, HR_j , and the new heart rate, HR , needed to correct the pressure.

The following equations give results similar to existing data on change in carotid pressure versus change in heart rate (Glick, 1965 and Robinson, 1966).

For $\Delta P_c \geq 0$

$$\Delta HR = e^{-a(\Delta P_c)} - 1 - (\Delta P_c)^{\frac{1}{b}} \quad (7)$$

For $\Delta P_c < 0$

$$\Delta HR = e^{-a(\Delta P_c)} - 1$$

Since changes in the partial pressure of CO_2 and O_2 also result in changes in heart rate, the equation must be amended to reflect this. For the blood gases and chemoreceptor reflex, similar normal operating values are set for the partial pressure of CO_2 , P_{CO_2j} , and the partial pressure of O_2 , P_{O_2j} . Subtracting these from their respective current values gives the change in partial pressure of O_2 , ΔP_{O_2} and the change in partial pressure of CO_2 , ΔP_{CO_2} . Including the blood gas effects into the equation above results in the following equation:

$$\Delta HR = e^{-a\Delta P_c} - 1 - \Delta P_c^{\frac{1}{b}} + C\Delta P_{CO_2} - d\Delta P_{O_2} \quad (8)$$

As described above, once the desired heart rate is known, then the forcing function can be adjusted to provide the proper heart durations and contractility.

The only remaining controlling mechanism is the vascular compliance, $K(V)$. After the other control mechanisms were changed accordingly, the vascular compliances and their rate of variability were found by making multiple computer simulations.

CONCLUSIONS

The pulmonary simulator has proved to work independently in evaluation of pulmonary mechanics and ventilation during whole body acceleration. The circulatory model and pulmonary model work in conjunction with each other as a single simulator. Inclusion of feedback mechanisms into the circulatory model improves its performance.

BIBLIOGRAPHY

- Ashman in Electrocardiographic Test Book, American Heart Association, Inc., 1956.
- Furnival, C.M., Linden, R.J., and Snow, H.M., Inotropic Changes in the Left Ventricle: The Effect of Changes in Heart Rate, Aortic Pressure and End-Diastolic Pressure. J. Physiol, 1970, 211, 359-387.
- Glick, G., and Braunwald, E. Relative Roles of the Sympathetic and Parasympathetic Nervous Systems in the Reflex Control of Heart Rate. Circulat. Res., 1965, 16, 363-375.
- Gregg, D.E., and Fischer, L.C. Blood Supply to the Heart. In Handbook of Physiology, Ed. by W.F. Hamilton and P. Dow. Am. Physiol. So., Washington, D.C., 1963, Section 2, Volume 2, pp. 1517-1584.
- Guyton, M.D. Textbook of Medical Physiology, W.B. Saunders Pub. Co., London-Toronto, 1971.
- Katona, P.G., Poitras, J.W., Barnett, G.O., and Terry, B.S. Cardiac Vagal Efferent Activity and Heart Period in the Carotid Sinus Reflex. American Journal of Physiology, 1970, 218, 1030-1037.
- Kezdi, P., and Geller, E. Baroreceptor Control of Postganglionic Sympathetic Nerve Discharge. American Journal of Physiology, 1968, 214, 427-435.
- Koch-Weser, J., and Blinks, J.R. The Influence of the Interval Between Beats on the Myocardial Contractility. Pharmacol. Rev., 1963, 15:601-652.
- Levy, M.N., Imperial, E.S., and Zieske, H., Jr. Ventricular Response to Increased Outflow Resistance in Absence of Elevated Intraventricular End-Diastolic Pressure. Circulat. Res., 1963, 12, 107-117.
- Rapela, C.E. and Green, H.D. Autoregulation of Canine Cerebral Blood Flow. Suppl. 1 to: Circ. Res., 14 and 15:205-211, 1964.
- Robinson, Brian F. Control of Heart Rate by the Autonomic Nervous System. Circ. Res., 1966, 19, 400-411.
- Rushmer, R.F. Effects of Nerve Stimulation and Hormones on the Heart; The Role of the Heart in General Circulatory Regulation. Handb. Physiol., 1962, sec. 2, vol. I, 533-550.
- Scher, A.M., and Young, A.C. Reflex Control of Heart Rate in the Un-anesthetized Dog. Amer. J. Physiol., 1970, 218, 780-789.

- Von Euler, U.S., Liljestrand, G., and Zotterman, Y. The Excitation Mechanism of the Chemoreceptors of the Carotid Body. Skand. Arch. Physiol., 1939, 83, 132-152.
- Wang, S.C. and Borison, H.L. An Analysis of the Carotid Sinus Cardiovascular Reflex Mechanism. Amer. J. Physiol., 1947, 150, 712-728.
- Warner, H.R. The Frequency-Dependent Nature of Blood Pressure Regulation by the Carotid Sinus Studied With an Electric Analog. Circ. Res., 1958, 6:35.
- Warner, H.R. and Cox, A. A Mathematical Model of Heart Rate Control by Sympathetic and Vagus Efferent Information. J. Appl. Physiol., 1962, 17, 349-355.

APPENDIX TO PART I

This appendix lists the subroutines and their purposes followed by a complete computer listing of the programs. The outlining of the subroutines will not include the details of the lung program. A flow chart describing the order of calculation is shown in Figure 27.

BMAIN - program of pumping heart and blood flow only

(circulatory portion of the model only)

BMAIN - calling routine controlling storage, subroutines, time incrementation, and I.O. Subroutines of **BMAIN**

BDRIVS - calculates flows, derivatives of volumes, and controls the leg valve.

RESIST - calculates resistance of all segments. Options available are $LOPR = \text{neg}$ makes $R = k/(V^2 + V)$. This is to model non-Newtonian flow in the capillaries if desired. Not presently in use.

$LOPR = 0$ makes $R = \text{constant}$

$LOPR = \text{pos.}$ makes $R = d/V^2$ in accordance with the Poiseuille-Hagen law.

PHEART - calculates the forcing function of the heart.

PCHART - calculates pressures and valve dispositions within the heart.

SKON - calculates compliance pressures. Options available are $LOPP1 = 0$ means compliance constant. $LOPP1 \neq 0$ makes compliance a function of volume. (See Appendix 1)

HAMING and **RUNGE** - calculates advancement of all independent variables in time.

Calling structure:

```

                                BMAIN
PHEART      RESIST      SKON      BDRIVS      HAMING      RUNGE
                                SKON      PCHART

```

BCC - program of gas exchange with constant blood flow

BCC - (same as BMAIN)

Subroutines of BCC

BCDRIV - calculates derivatives of tissue concentrations.

Options are:

LOPGS = 1 execute for only the gases O_2 and CO_2

LOPGS = 2 execute for only the gases O_2 , CO_2 , and X

LOPGS = 3 execute for only the gases X

LOPGS = 4 execute for only the gases O_2 , CO_2 , and CO

LOPGS = 5 execute for all the gases O_2 , CO_2 , CO, and X where

X is one or more gases that do not bind to hemoglobin

O2DRIV - calculates the $\frac{dP_{O_2}}{dt}$, $\frac{dP_{CO_2}}{dt}$, and $\frac{dP_{CO}}{dt}$ for all chambers. ($\frac{dP_{CO}}{dt}$ is not calculated if LOGS.LT.4).

XDRIV - calculates the $\frac{dx}{dt}$ for all chambers (is not called unless LOGS = 2, 3, or 5)

SATUR - calculates S_{O_2} , C_{CO_2} , $\frac{dS_{O_2}}{dP_{O_2}}$, $\frac{dS_{CO_2}}{dP_{CO_2}}$, $\frac{dC_{CO_2}}{dP_{O_2}}$, and $\frac{dC_{CO_2}}{dP_{CO_2}}$.

GFLTST - calculates K_{O_2} and K_{CO_2} for all chambers.

FLTEST - determines the direction of flow and $(C_v)^{in}$ and $(C_v)^{out}$ for each chamber.

Calling Structure

		BCC	
	BCDRIV		Subroutines of BMAIN
	O2DRIV	XDRIV	
SATUR	GFLTST	GFLTST	
	FLTEST	FLTEST	

BCMAIN program of gas exchange with pumping heart (circulatory model with gas transport)

BCMN - same as BMAIN.

Subroutines of BCMAIN consist of all those in BMAIN plus all those in BCC.

MAIN complete cardio-pulmonary model to date.

MAIN - controls the execution of the blood program (BCMAIN) and lung program (LMAIN) so that they may be executed with different time steps and durations.

Subroutines in MAIN.

BCMAIN - circulatory model with gas transport with various entry points added.

LMAIN - complete lung program with various entry points added.

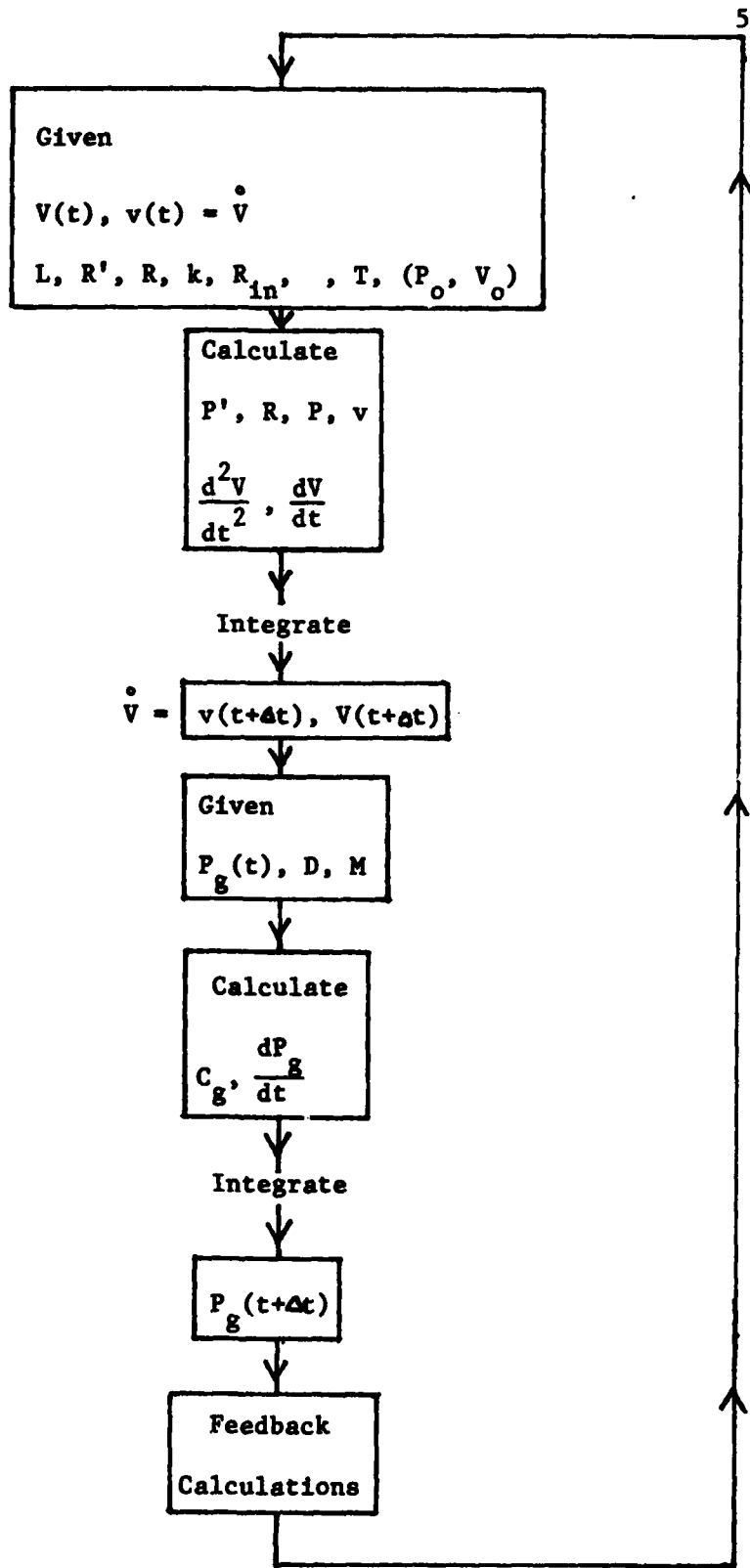
BLCONV - calculates the rate of removal of each gas from each alveoli chamber.

LBCONV - calculates external pressures on blood chambers using alveoli pressures and pleural pressures from the lung

program and converts each gas concentration to each gas partial pressure in each alveoli.

Calling Structure

		MAIN		
BCMAIN	LMAIN	BLCONV	LBCONV	



The order of calculation within the program.

Figure 27

PART II

DEVELOPMENT OF A NONINVASIVE METHOD FOR DETERMINING
LUNG VENTILATION DISTRIBUTIONS WITH THE AID OF A
NUMERICAL SIMULATOR OF THE HUMAN PULMONARY SYSTEM

I. INTRODUCTION

There are numerous techniques for diagnosing and analyzing lung diseases which cause uneven ventilation. These can involve a wide variety of medical diagnostic techniques ranging from the common chest x-ray to the more elaborate technique of fiberoptic bronchoscopy. This report presents a new method for diagnosing and analyzing lung diseases which cause uneven ventilation. This new method is considered advantageous relative to most other methods for three main reasons: it is noninvasive, it is relatively inexpensive to use, and it can be performed in a relatively short period of time. Before describing this new method some of the other methods currently used for diagnosing lung disease are reviewed below for later comparison with the new method introduced. This is preceded by a brief explanation of pulmonary ventilation and associated diseases.

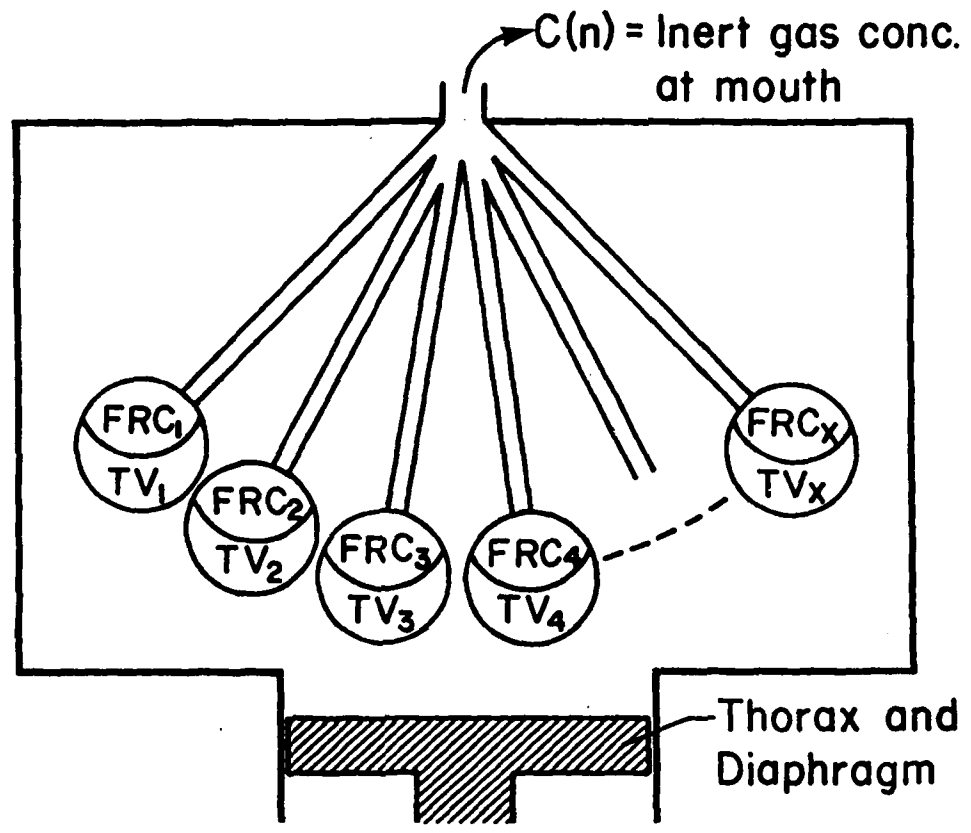
The most important function of the lungs is to ventilate the alveoli, the functional units of the lung parenchyma, for the purpose of gas exchange with the blood. Thus, tissues of the body are supplied with oxygen and relieved of carbon dioxide. Lungs also eliminate waste in vapor or gas form and serve as a blood reservoir for controlling fluctuations in extrapulmonary blood volume and pressure. The volume ventilating the lungs each breath is approximately equal to the volume, known as the tidal volume (TV), entering the nose and mouth during each breath with some correction due to changes in

temperature and water vapor pressure as air enters the lungs. If ideal ventilation were to occur inspired air of the same composition would be distributed uniformly to each of the parenchymal units, each unit receiving an equal fraction of its preinspiratory volume. In reality ideal ventilation does not occur, even in healthy persons. However, certain environmental factors and disease states can cause extremes in the imbalance of ventilation of different parts of the lungs. Asthma, emphysema, bronchitis, and tumors cause uneven ventilation. Changes in whole body acceleration, such as that experienced by astronauts and pilots of high performance aircraft, frequently have detrimental effects on regional pulmonary ventilation that may contribute to impairment of abilities to function physically and mentally (Burton, et al., 1976). In all cases of uneven ventilation the result is impaired or ceased function of the poorly ventilated lung regions.

A number of techniques are presently used for analyzing pulmonary ventilation. In clinics and pulmonary function laboratories the techniques primarily used include the inert gas washout test, the helium distribution test, the single breath oxygen test, and bronchiospirometry (Comroe, et al., 1962). Each of these techniques may be utilized to augment an examination of regional lung function. However, of these methods only bronchiospirometry provides a means for analyzing regional ventilation, and this is only a gross analysis. It aids only in distinguishing the ventilation of the major divisions of the lungs by catheterization of one or both of the main bronchi. None of these methods provides a means of analyzing the ventilation characteristics within a region smaller than the two major divisions.

Some of the techniques used in research provide a more detailed assessment of regional ventilation of the lung. The volume of gas in poorly ventilated or unventilated alveoli can be calculated by using the body plethysmograph to measure the total volume of gas in the thorax and subtracting from this the volume measured by a technique that washes out only alveolar gas in communication with airways (Comroe: *Physiology of Respiration*, 1974). A commonly employed method of determining regional ventilation is performed by measuring regional clearances of inhaled Xenon-133, or other radioactive gas, using externally positioned scintillation detectors (Schmid, et al., *Jap*, 49:279-286, 1980; Rehder, et al., *Jap*, 42:391-402, 1977; Dolfuss, et al., *Respir. Physiol.*, 2:234, 1967). In a similar method Xenon-133 dissolved in saline is injected intravenously, and the washout of this poorly soluble gas is measured with external detectors as it diffuses into the alveoli (Dollery and Hugh-Jones, *Brit. Med. Bull.* 19:59, 1963). Another more accurate method is the use of fiberoptic bronchoscopy arranged for sampling gasses at specified locations within the bronchial tree (Denison, et al., *Resp. Physiol.* 42:87-99, 1980).

The research methods discussed above are used to determine whether uneven ventilation is occurring and approximately to what extent it is occurring. However, of these methods only the radiographic techniques and the recently tested fiberoptic bronchoscopy provide information regarding the locations of the poorly ventilated regions. Experiments with various research laboratory techniques occasionally provide new approaches for estimating regional lung ventilation, but few of the research techniques currently used are



Parallel Ventilation

(D. M. Gomez, P.N.A.S. 49:312, 1963)

Figure 1 Schematic of the Gomez Ventilation Model

rapid methods employing safe, noninvasive procedures appropriate for clinical application.

The initial objective of this work is to introduce a noninvasive technique for the indirect determination of the distribution of ventilation within the lungs from gas concentrations in expired air measured at the mouth. It is believed that such a technique can be further developed as a noninvasive procedure for determining regional ventilation.

The idea that changes in the distribution of ventilation within the lungs can be determined from the record of changes in concentrations of test gas in expired air measured at the mouth is not a new concept. Domingo M. Gomez proposed such a technique in previous reports (Gomez, 1962, 1963), but because of limitations of his method it has not been widely used. Gomez proposed treating the lungs as a continuous collection of volume units with parallel ventilation, with each unit having some value for ventilation, Z , defined as the ratio of tidal volume to functional residual capacity. This model is shown schematically in Figure 1. Using this assumption Gomez showed that, for washout of a non-diffusing gas, the graph of expired concentration, $C(N)$, versus number of breaths, N , was uniquely determined by the distribution, $F(Z)$, of ventilation in the lungs. In other words each volume element of the lungs has a value for the ratio Z , and $F(Z)DZ$ is the fraction of all chambers having values for this ratio between Z and $Z+DZ$. Gomez then showed that one could determine the graph of $F(Z)$ versus Z for a subject from the graph of $C(N)$ versus N obtained in an inert gas washout test as shown in Figure 2.

PROCEDURE

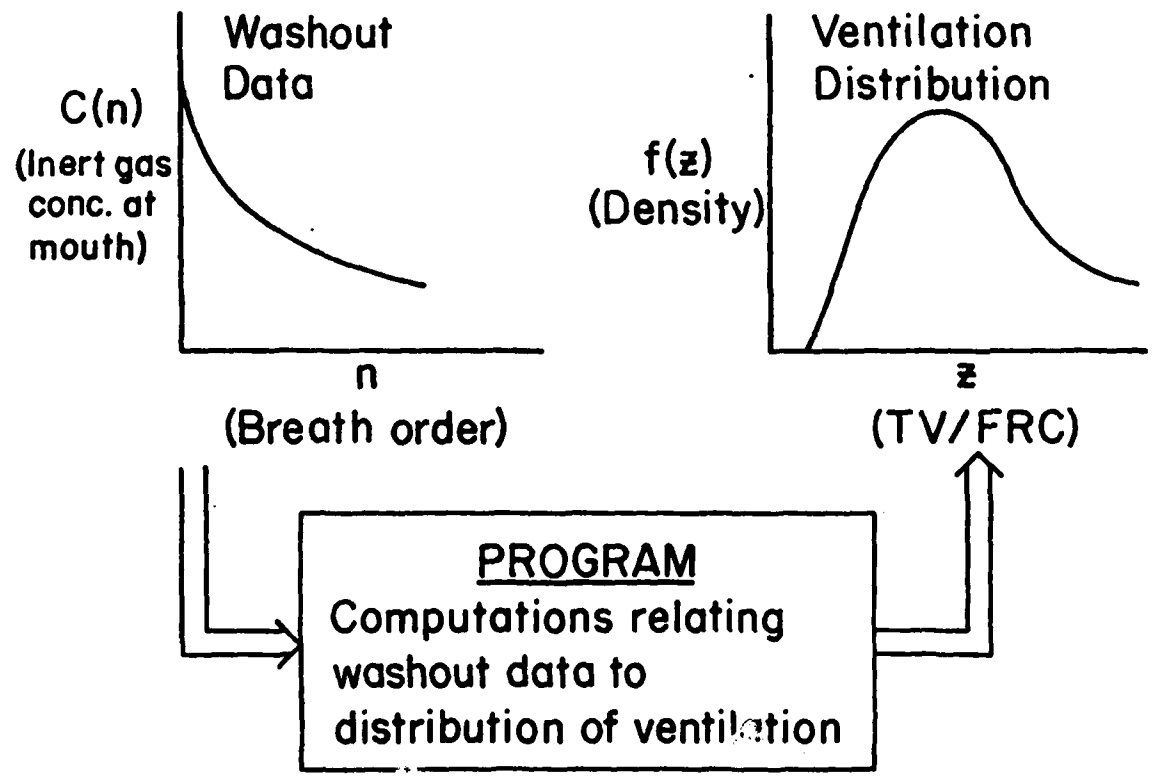


Figure 2 Computational Scheme in the Gomez Model

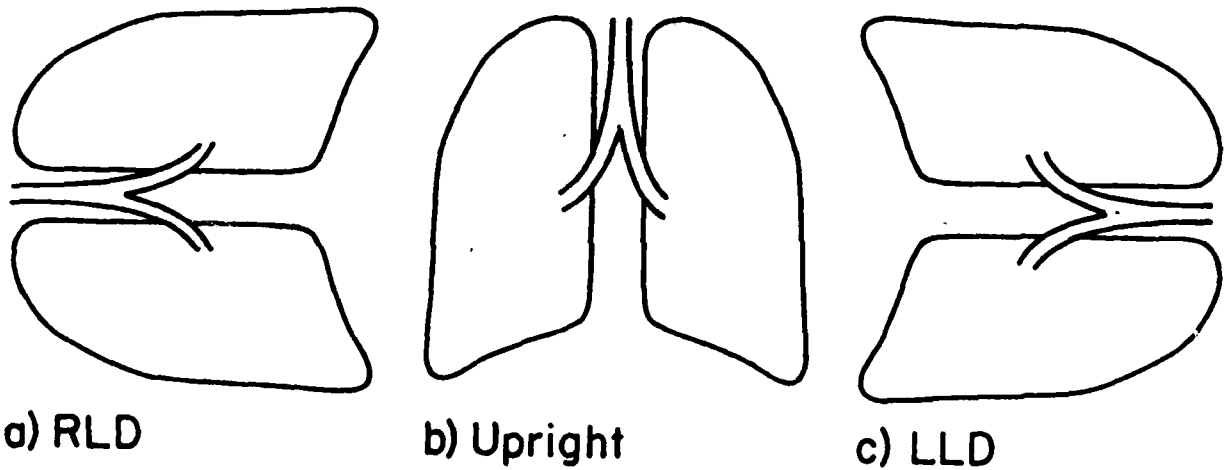
The Gomez method of calculating $F(Z)$, ventilation distribution, from $C(N)$, expired gas concentrations measured at the mouth, has been used to compute the distribution of ventilation in the lung even though the actual lung is not ventilated exclusively in parallel, as in the Gomez model. Thus the computed distribution, $F(Z)$, is the equivalent distribution that parallel ventilated lungs would need in order to function as the actual system with respect to ventilation. Denison, et al. (Resp. Physiol. 42:87, 1980) used information from lung gas samples taken from inside the lung via bronchoscopy to demonstrate changes in regional ventilation resulting from changes in body position as indicated in Figure 3. Hence, changes in the graph of $F(Z)$ versus Z with change in body position may be interpretable. In fact, it may be possible to determine not only the fractional distribution of ventilation but also to determine which spatial regions have large or small ventilation solely by this noninvasive method simply by examining changes in concentrations of expired gasses resulting from changes in body position.

The suggested procedure is to compute the ventilation distribution, $F(Z)$, from expired gas concentration, $C(N)$, at a given body position. Then change the body position and repeat the run. This is repeated for a number of body positions to produce a family of ventilation distribution curves computed for a particular subject. It is anticipated that changes in the general pattern formed by this family of curves can be correlated with changes in regional ventilation in the lungs, as indicated in Figure 4.

A computerized simulator for the human lungs is being used for this research. A number of mathematical simulators have been

Analyzing Regional Ventilation Dysfunctions:

Change in position → Change in $f(z)$ vs z



(D. M. Denison et al., Resp. Physiol., 42 : 87-99, 1980)

Figure 3 Conceptualization of Denison et al. Ventilation Test

II. Application of Technique

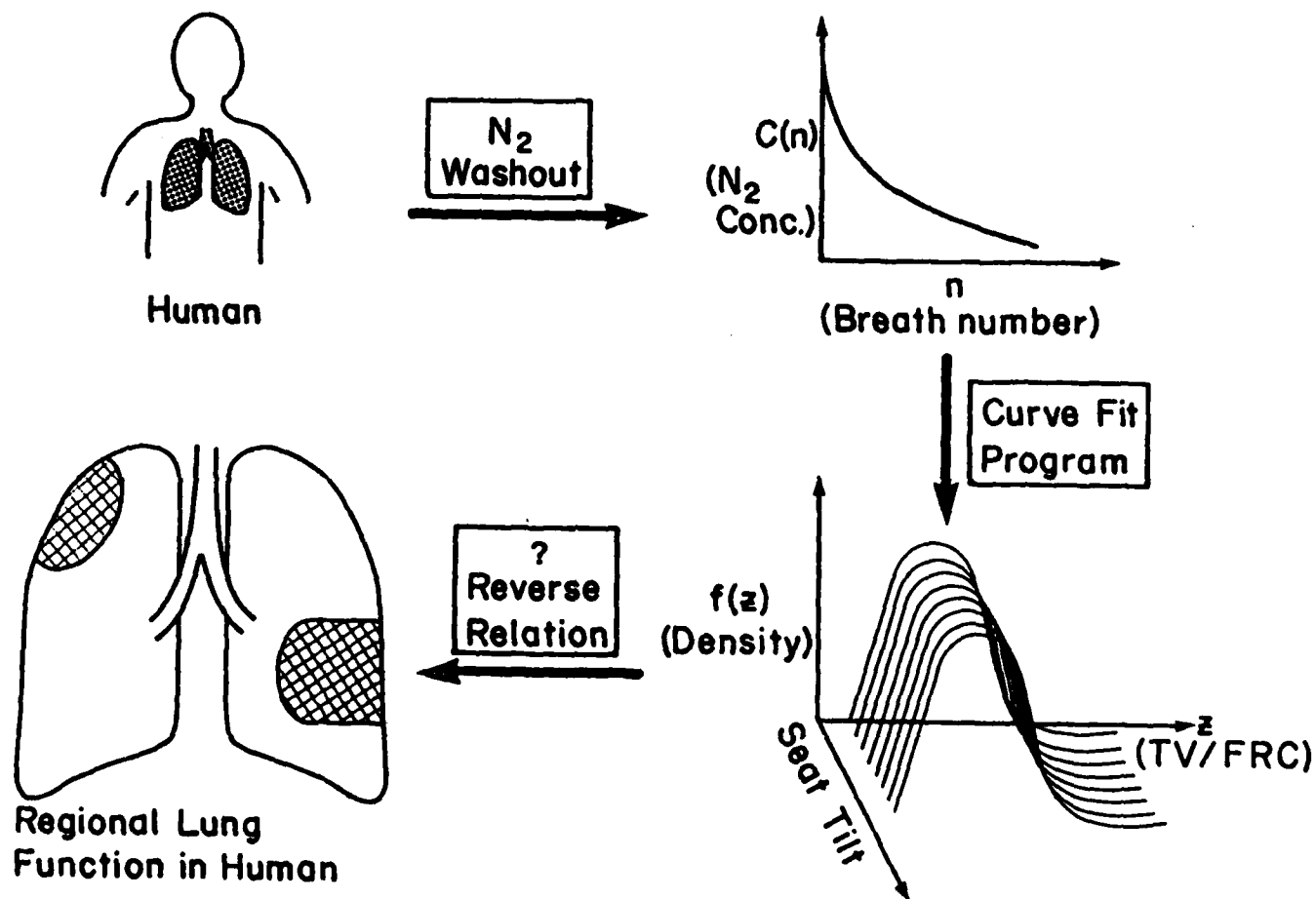


Figure 4 Conceptualization of Method for Determining Local Ventilation Dysfunctions

developed for modeling the lungs (Collins, 1967; Grimby, et al., 1968; Saidel, et al., 1971; Lambert and Wilson, 1973; Fry and Hyatt, 1960; West, 1969; Mead, et al., 1970; Saidel, et al., 1972; and Hilberman, et al., 1973). One that serves as a more complete numerical simulator of the human pulmonary system has been recently developed (Calvert, 1980). A version of this computerized model has been used to provide inert gas washout data for this research. The model provides a convenient means for performing experimental trials for this investigation, because known variations in regional ventilation can be programmed to the model as well as changes in body position and whole body acceleration. Clinical tests have yet to be performed to provide inert gas washout data from subjects with known regional lung characteristics to verify the methods. This concept is illustrated in Figure 5.

The research plan included the following:

- 1) The algorithm of the computerized numerical simulator of the lungs was amended so that it provided data simulating a multi-breath inert gas washout test.
- 2) A companion program named N2WASH was written that retains values for breath order N and mean concentration $C(N)$ of inert gas in expired air of each breath. This program also uses data from the lung model to determine the tidal volume, TV , and functional residual capacity, FRC , of each breath during the simulated inert gas washout.
- 3) The best fit for a curve of $C(N)$ versus N was computed, and the data from this curve was used to compute the distribution, $F(Z)$, of ventilation, TV/FRC . At this point in the investigation a flaw was discovered in the numerical methods used to compute the ventilation distributions using parameters computed from the numerical approximation of the nitrogen washout curve. (An explanation of this flaw in the methods is provided below.) The body position simulated in the lung model was changed and the washout test repeated. Computation of a distribution was planned for each body position, and thus a profile of distributions would be established to characterize the lungs simulated.

I. Development of Technique

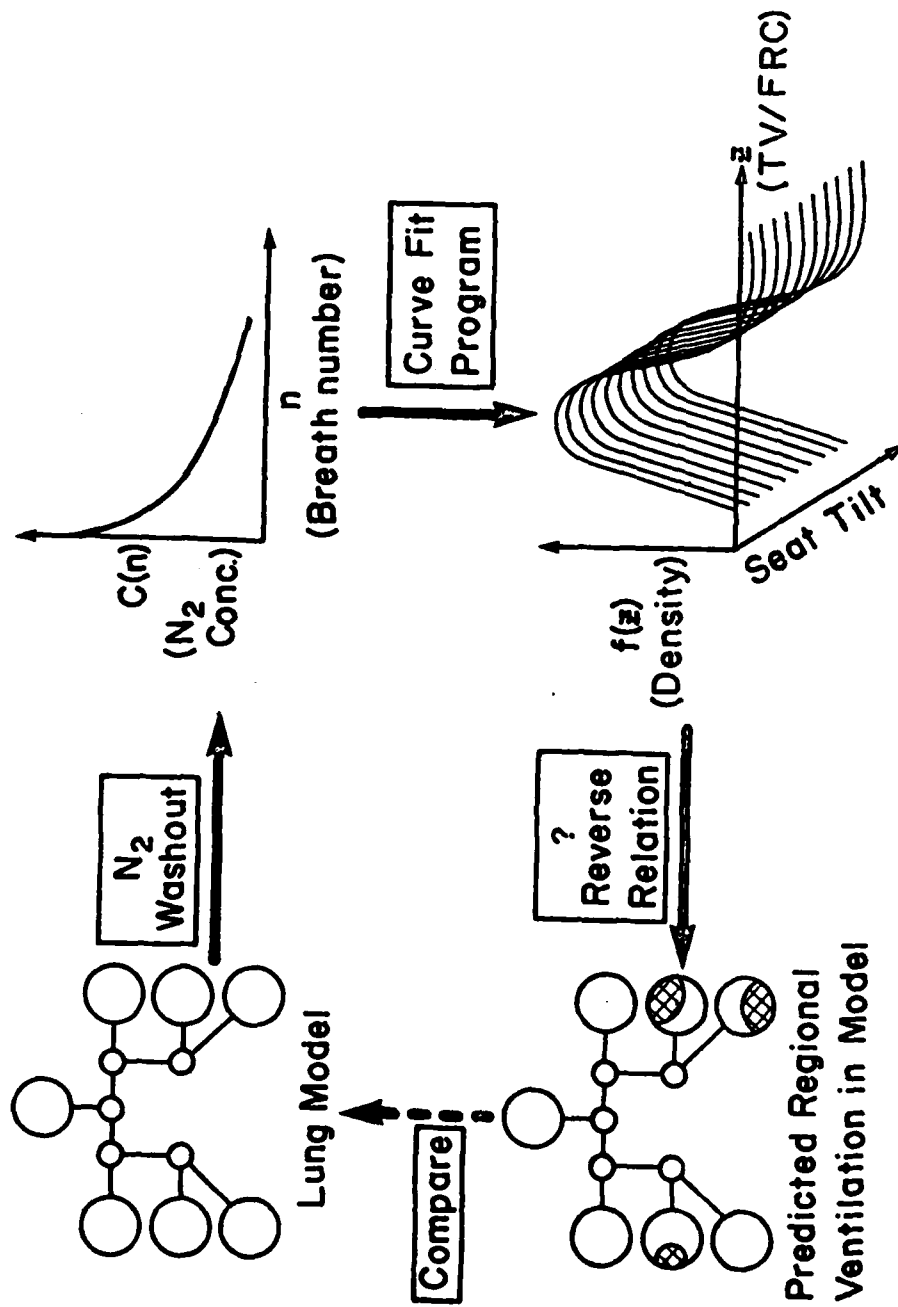


Figure 5 Simulation Plan to Validate Non-Invasive Method of Determining Local Ventilation Dysfunctions

- 4) Step 3 was to be performed with simulated normal lungs and with regional ventilation dysfunctions programmed into the lung model. The completed procedure was expected to provide a separate profile of distributions, $F(Z)$, representing each different ventilation dysfunction. The most critical part of this step would be to determine a relation between the computed distributions $F(Z)$ and corresponding regional ventilation patterns that allow accurate prediction of these patterns.

It was discovered that the flaw in the numerical methods lay in the equation used to approximate the nitrogen washout curve. This equation, a sum of exponential terms, was sensitive to error in initial approximations of the curve fitting parameters. In order to obtain parameters which provided a reasonably close approximation to the expected ventilation distribution, the initial estimates of parameters for the curve-fitting equation had to be very close to the final values computed with an iterative least squares procedure. Otherwise the computations failed to close in on acceptable parameter values, or a large and costly number of iterations was required to close in on acceptable values for the parameters. The flawed iterative procedure was the application of the afore-mentioned Lagrangian method of undetermined multipliers used for minimization in a least squares procedure. During each iteration new values were selected for the curve fitting parameters using an interval halving approach.

Recently an alternative method for approximating lung ventilation distribution curves has been developed. This alternative procedure is described below in a subsequent portion of this report. At present this alternative procedure is being implemented for achieving the ultimate goal of this investigation, that of developing a noninvasive procedure for determining the locations of localized or regional dysfunctions within the lungs.

Development of a noninvasive method of characterizing ventilation distributions could lead to a useful tool for clinical applications. In particular this method may be useful in diagnosing regional ventilation dysfunctions such as occur with emphysema, fibrosis and tumors.

II. EQUATIONS AND COMPUTATIONS METHODS

A. Mathematical Methods

The initial goal of this research, as stated in the introduction, is to develop a numerical method for determining the ventilation distribution in the human lungs. The suggested procedure requires the measurement of end-expiratory nitrogen concentrations taken at the mouth during a nitrogen washout procedure. The next step in determining the ventilation distribution is to fit the nitrogen washout data with an equation for the nitrogen washout curve. This curve-fitting is performed by a least squares procedure. However, this procedure is complicated by two constraints imposed by the Gomez equations (Gomez, 1963) used in this investigation for determining the ventilation distribution. The curve fitting equation and the two constraint equations are given below.

The curve to fit is:

$$C(N) = VL/VT * [\text{SUM OVER } J=1, NP] A(J) \left(\frac{1}{(B(J,L) - 2+N)^{(M(J,L)+1)}} - \frac{1}{(B(J,L) - 1+N)^{(M(J,L)+1)}} \right) , \quad N = 1, 2, \dots, NBO. \quad [1]$$

The two constraints are:

$$1 = [\text{SUM OVER } J=1, NP] A(J) (1 / ((B(J,L) - 1)^{(M(J,L)+1)})) \quad [2]$$

and

$$\begin{aligned} VT/VL = [\text{SUM OVER } J=1, NP] A(J) & ((1 / ((B(J,L) - 2)^{(M(J,L)+1)})) \\ & - (1 / ((B(J,L) - 1)^{(M(J,L)+1)}))) \quad [3] \end{aligned}$$

The two constraint equations require the use of Lagrange's method of undetermined multipliers along with the least squares procedure to select parameters for the best fitting washout curve. The parameters selected in this fashion are given values which are useful also in constructing the ventilation distribution curve.

The least squares method, applied in conjunction with Lagrange's method for unknown multipliers is used to find the values for the parameters A(J) which provide the best fitting approximation for the washout curve. This least squares approach generates a number of simultaneous equations which are solved later in a subsequent elimination routine. The coefficient and solution matrices used in the elimination are established in the program CRVFIT (see section below on program CRVFIT) as follows:

```

*****                               *****   *****   *****
* D(1,1)A(1)   D(1,2)A(2)  ---- D(1,NP+2)A(NP+2)  *   * P(1)   *
* D(2,1)A(1)   D(2,2)A(2)  ---- D(2,NP+2)A(NP+2)  *   * P(2)   *
* -           -           ---- -                 * = * -     *
* -           -           ---- -                 *   * -     *
* D(NP+2,1)A(1) ----- D(NP+2,NP+2)A(NP+2) *   * P(NP+2) *
*****                               *****   *****   *****

```

where NP is the number of independent variables A(J), and NP+2 is the total number of variables A(J) including the two variables (two Lagrangian undetermined multipliers) determined by the two constraint equations. The D(I,J) are constants derived in the least squares procedure. The first two rows contain coefficients corresponding to constraint equations and should be placed at the top of the matrix, because the last two coefficients in these rows are zero. The elimination routines require that no zeroes lie on the diagonal. The constants P(J) represent the data vector.

Initial values for parameters M(J,L) and B(J,L) must be input by the user. The minimum dimension required for subscript J in both M(J,L) and B(J,L) is two less than the number of unknown parameters A(J) used in the curve fitting process.

The equation for the curve to fit, shown above, is derived from mass balance equations for a nitrogen washout procedure. In the process of constraining the mass balance equations to accommodate the requirements described by D.M. Gomez (Gomez, 1963) for determining the ventilation distribution, the following conversion was made for convenience in deriving those mass balance equations:

$$U = \text{LN}(1+Z)$$

Here Z represents the ratio of TV/FRC for a ventilating unit in the lungs. Using this conversion the following model was derived for the ventilation distribution:

$$F(Z) = F1(U)$$

$$F_1(U) = [\text{SUM OVER } J] (A(J)/M(J,L!)) * (U^{**M(J,L)}) * \text{EXP}(-B(J,L)U)$$

Initial values for the constants M and B are chosen in the following manner:

The constants M(J,L) and B(J,L) are chosen such that the plot of fractional distribution of ventilation F(Z) versus ventilation Z of healthy normal lungs assumes the expected narrow unimodal shape (S.M. Lewis, et al., 1978). These constants can be selected by the following procedure: a point is selected from the distribution curve where the distribution of Z (Z = TV/FRC) is expected to fall to a negligible value. For example it may be that Z were rarely expected to be 10 or greater under experimental conditions. Therefore, M and B may be chosen such that the value for F(Z) at the point where Z = 10 is negligible relative to the maximum value for F(Z). The maximum value for F(Z) corresponds to the Z value where D/DZ F(Z) = 0 or to the U value where D/DU F₁(U) = 0. Assuming one variable term A(J) is used,

$$F(Z) = (A/M!) ((\text{LN}(1+Z))^{**M}) \text{EXP}(-B(\text{LN}(1+Z))) \quad \text{or}$$

$$F_1(U) = (A/M!) * (U^{**M}) * \text{EXP}(-BU)$$

setting $D/DU F_1(U) = 0$

yields $U = M/B$

Therefore, $U = M/B$ at the point of maximum distribution $F_1(U)$. Thus, for negligible F(Z) at Z = 10:

$$[F(Z) \text{ at } Z = 10] \quad [F(Z) \text{ at max } (U = M/B)]$$

or, as an example, let

$$\begin{aligned} [F(Z) \text{ at } Z = 10] / [F(Z) \text{ at max } (U = M/B)] &= 0.01 \\ (A/M!) (U^{**M}) \text{EXP}(-BU) / (A/M!) ((M/B)^{**M}) \text{EXP}(-M) &= 0.01 \end{aligned}$$

this yields

$$\text{EXP}(M-BU) * ((BU/M)^{**M}) = 0.01 .$$

For $Z = 10$, $U = \text{LN}(11)$. Thus the appropriate values for M (values for M which are expected to provide the narrow unimodal shape previously mentioned) may be chosen arbitrarily and the corresponding values for B found by trial and error.

It was noted that values chosen for the constants $M(J)$ and $B(J)$ should be selected such that the different ratios $M(J)/B(J)$, the ratios representing the values for Z where $F(Z)$ is at a maximum, are different enough to allow for the sum of widely spaced curves summed to fit the data.

B. Mainframe System and Language Used

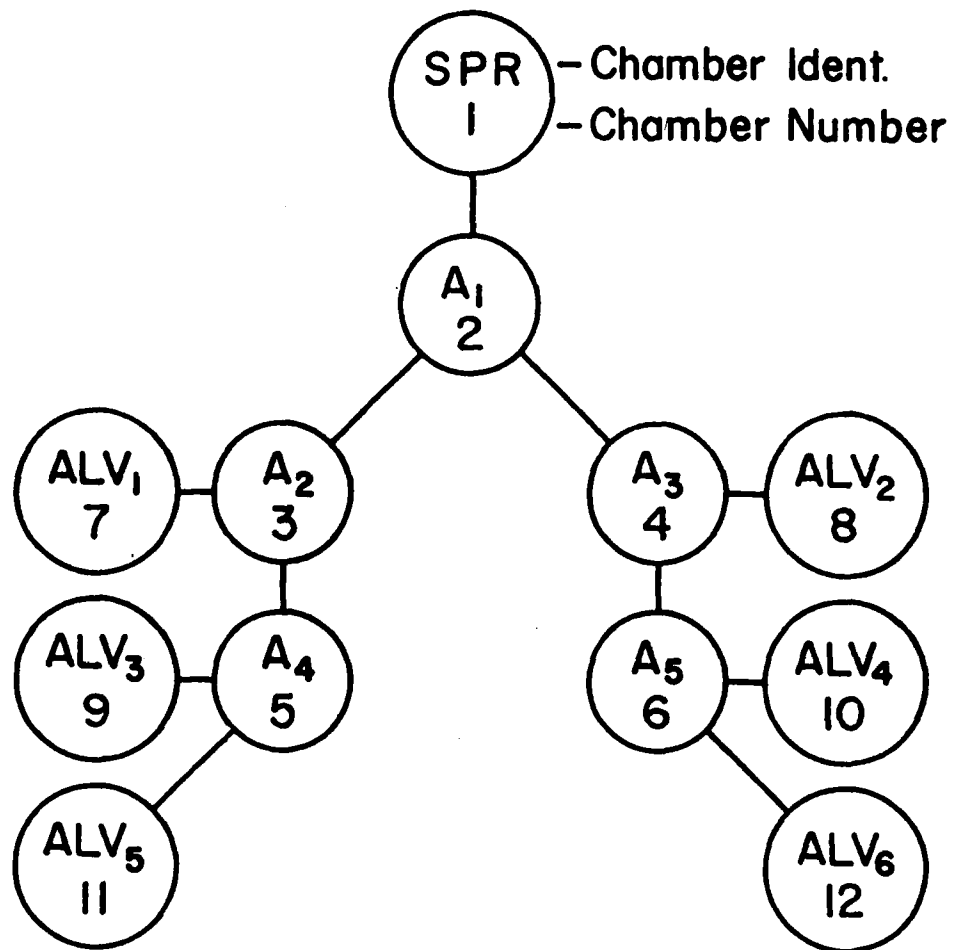
The computer language used for this project was the most current version of Fortran available at the University of Texas, Fortran 77. The compiler used was the FTN5 compiler. This was the one compiler available at the university providing compiled versions of Fortran programs which allowed the most rapid execution on the mainframe computer system. The mainframe system maintained by the Computation

Center at the university was a Control Data Corporation 6600 Digital Computer.

C. The Lung Model

***** Program LUNG *****

Program LUNG is a numerical simulator of the human pulmonary system written in Fortran. This simulator was developed by Ray E. Calvert (1977, 1980) in his research efforts for both the Masters and Doctoral degrees in biophysics. This research was performed under the supervision of R. Eugene Collins, Professor of Biophysics at the University of Houston. The model provides a dynamic mathematical representation of the pulmonary structures and their functions during respiration, including the gross pulmonary structural mechanics, mechanics of airflow in the lung airways, and ventilation of major lung regions. The model shown schematically in Figure 6 is composed of six alveolar chambers representing the alveoli or acini ventilated through five airway chambers representing the bronchial tree. These airways interconnect the alveolar chambers in an arrangement that provides both parallel and series ventilation of the alveolar chambers. In addition there is a twelfth chamber representing a spirometer which is used as the sole source of gasses inspired. The diaphragm and abdominal and thoracic respiratory muscles are modeled as a system of pistons which provide the driving forces of inspiration and expiration. The model includes the fluid pressure within the chest and abdominal cavities resulting from gravitational forces on the thorax, diaphragm and abdomen. The model also simulates the hydrostatic pressure gradient within the pleural fluid and the effects



Parallel and Series
Ventilation

Figure 6 Schematic of Ventilation Compartments in Pulmonary Simulator

it has upon the regional lung volumes. Variations in the magnitude of the gravitational field and in the orientation of the lungs within the field are simulated by the model. A more detailed description of this model is given in previous AFOSR reports on this project.

The main program coordinates 19 subroutines. All are controlled by 22 input options which allow the user to orchestrate execution, input, and output such that innumerable combinations of lung type, inspired gasses, and breathing dynamics can be modeled.

D. Companion Programs for Data Processing

***** Program LUNGID *****

Program LUNGID is another program written by Calvert (1980) to organize data output by program LUNG. This program reads a file on which data from program LUNG have been stored and organizes and outputs those data in readable form. It provides large volumes of detailed data pertaining to a great number of the mechanical and quantitative changes in the lungs that occur during breathing. This is helpful when diagnosing execution errors.

***** Program N2WASH *****

This program reads data from a file output by program LUNG and selects and prints only output pertinent to nitrogen washout studies. Program N2WASH also outputs data to another file to be used later for the purpose of curve-fitting data to an equation for the nitrogen washout curve and eventually for the purpose of computing ventilation distributions.

E. The Curve-Fitting Programs

***** Program CRVFIT *****

This program selects data from a nitrogen washout procedure and computes a best fit curve for the nitrogen washout data. The equation used to construct this curve is an exponential equation with parameters selected to conform to constraints imposed by the Gomez equations (Gomez, 1963) for determining the ventilation distribution. Lagrange's method of undetermined multipliers is used here in conjunction with a least squares approach for fitting a curve with two constraints. Thus parameters selected for the best fitting washout curve possess values also suitable for later use in the construction of a ventilation distribution curve. As explained below in the section on program VDPLLOT ventilation distribution curves are subsequently used for characterizing the lungs tested. The washout curve is $C(N)$ versus N where $C(N)$ represents the average concentration of nitrogen in the lungs at the end of breath number N . The equations for the curve to be fitted to the washout data are repeated here for convenience:

The curve to fit is:

$$C(N) = VL/VT * [\text{SUM OVER } J=1, NP] A(J) \left(\frac{1}{(B(J,L) - 2+N)^{M(J,L)+1}} \right) - \left(\frac{1}{(B(J,L) - 1+N)^{M(J,L)+1}} \right) , \quad N = 1, 2, \dots, NBO. \quad [1]$$

The two constraints are:

$$1 = [\text{SUM OVER } J=1, NP] A(J) \left(\frac{1}{(B(J,L) - 1)^{M(J,L)+1}} \right) \quad [2]$$

and

$$VT/VL = [\text{SUM OVER } J=1, NP] A(J) \left(\frac{1}{(B(J,L) - 2)^{(M(J,L)+1)}} \right) - \left(\frac{1}{(B(J,L) - 1)^{(M(J,L)+1)}} \right) \quad [3]$$

An iterative procedure has been developed for finding the optimal values for the parameters $M(J,L)$, $B(J,L)$, and $A(J)$ for the nitrogen washout curve approximation. The following procedure is used: initial values for parameters M and B are selected. Using these values the values for the corresponding $A(J)$ are computed. The corresponding washout curve $CEQ(L,N)$ is computed and compared with the data values $C(N)$ for the washout. The average of the absolute values of the deviations of the computed values, $CEQ(L,N)$, from the observed values, $C(N)$, is computed each iteration. This average deviation is labelled $SD(J,L)$. One of the values for M or B is temporarily incremented, and a new washout curve and $SD(J,L)$ are computed. If the $SD(J,L)$ increases, indicating an increase in error, a change in the most recently altered parameter, M or B , is selected to be $-\frac{1}{2}$ times the previous change, i.e.,

$$DM(J,L) = -\frac{1}{2} * (DM(J,L - 1))$$

or

$$DB(J,L) = -\frac{1}{2} * (DB(J,L - 1))$$

However, if the $SD(J,L)$ decreases initially a change in the parameter M or B is selected to be twice the previous change:

$$DM(J,L) = 2.0 * DM(J,L - 1)$$

or

$$DB(J,L) = 2.0 * DB(J,L - 1)$$

Use of this interval-doubling process is continued with each parameter for which incrementation has resulted in a decrease in average deviation, $SD(J,L)$. After an incrementation results in an increase in average deviation, from that time onward an interval-halving routine is employed until the desired accuracy is achieved or until the time limit provided by the user is exceeded. If the $SD(J,L)$ decreases while using this routine without interval-doubling, the subsequent change in the parameter M or B is selected to be identical to the previous change:

$$DM(J,L) = DM(J,L - 1)$$

or

$$DB(J,L) = DB(J,L - 1)$$

This process of choosing parameters such that the average deviation, $SD(J,L)$, decreases is continued until the average deviation is less than or equal to an arbitrarily selected maximum called $SDMAX$. When the average deviation becomes smaller than this arbitrarily chosen value the approximated washout curve is considered to be an adequately accurate fit and may be used in obtaining information about ventilation distribution. This information is subsequently used to extract information concerning regional function in the lungs.

***** Program FAMZ *****

Program FAMZ has two different uses. One is to plot data on a Diablo Teletype terminal. Thus clinical washout data or modeled washout data may be compared graphically with computed washout data provided from program CRVFIT. These data are compared by plotting all curves on the same graph. This is convenient when the user wishes to obtain a graphical comparison for visualizing the closeness of fit of an approximated curve to the curve being fitted.

The second use of Program FAMZ is to compute and plot washout concentrations for up to five different washout curves on a single graph. These curves are computed within program FAMZ from the washout curve equation with parameters input by the user. This use of program FAMZ provides a tool by which one may familiarize oneself with the graphing characteristics of the equations used to approximate the changes in expired nitrogen concentration observed in a nitrogen washout procedure. These equations are provided in the section above on program CRVFIT.

The approach to familiarization is to execute this program a number of times changing the value of one of the parameters $M(J)$ and $B(J)$ before each execution while keeping other parameters constant. According to the curve fitting equations the $A(J)$ depend upon the $M(J)$ and $B(J)$ chosen. During each execution a fitted washout curve of $CEQ(L,N)$ versus N is plotted to provide a visual means by which to judge the effects of the changes employed. This is done with the Hyplot Plotting Routine provided as a library program by the University of Texas for creating graphs with a Xerox Diablo Computer terminal. These graphs using arbitrarily chosen parameters may be compared to

graphs of clinical washout data from normal healthy individuals or graphs of data from the lung program to determine what values for the curve-fitting parameters may be considered appropriate for modeling the washout of normal lungs.

This is not an accurate test of the effects of the parameters $M(J)$ and $B(J)$ computed by program CRVFIT, because the $A(J)$ are not accurately computed. The $A(J)$ are kept constant for each set of parameters. This allows investigation of the effects of the varying parameters $M(J)$ and $B(J)$ on the plots without interference from changing $A(J)$. To visualize the washout curve resulting from more accurately computed parameters from program CRVFIT, all three sets of parameters, $M(J)$, $B(J)$, and $A(J)$ are input by the user. To do this a read statement is used in program FAMZ to input the $A(J)$, and the code used to compute the $A(J)$ is by-passed.

F. Computing the Ventilating Distribution

***** Program VENDIS *****

This program reads the washout curve-fitting parameters, $M(J)$, $B(J)$, and $A(J)$, from an input file created in program CRVFIT and uses the ventilation distribution equation to compute the ventilation distribution for the particular lungs which were used to obtain the curve-fitting parameters. The equation for ventilation distribution is

$$F(Z) = [\text{SUM OVER } J=1, NP] A(J)/M(J)! * [(LN(1+Z))^{**M(J)}]/(1+Z)^{**B(J)}$$

Finally the arbitrarily chosen data points for ventilation, Z , and the corresponding ventilation distributions, $F(Z)$, computed in program VENDIS are stored on an output file for later use in the plotting routine, VDPLOT.

This program uses the IMSL routine gammas, which computes the gamma function for given input values. The gamma function is used to compute the factorial function of the parameters $M(J)$.

***** Program VDPLOT *****

This program reads and plots ventilation distribution data using the Hyplot routine for plotting graphs with a Diablo terminal. There are as many as 24 sets of washout data for each individual set of lungs examined. These correspond to the 24 different seatback angles used for the washout test. For a simultaneous plot of all ventilation distributions for a particular set of lungs this program requires that data files for all seat tilts for a particular set of lungs, up to 24 files, be copied to a single file. The value for NPLOTS, the number of graphs to be plotted, must also be entered on the input file.

The programming included in this routine alters input data such that each distribution curve is slightly offset from the previous one. This provides a three-dimensional effect or a perspective view of the curves. All the curves thus plotted together can be visualized as the framework of a surface. The appearance of this framework may be used to suggest the physical characteristics of the lungs it represents, especially uneven ventilation within different regions of the lungs.

G. Alternative Method for Computing Ventilation Distribution

A fifty-compartment, numerical model employed by Wagner, et al. (1974) to compute distributions of ventilation-perfusion ratios provides an algorithm adaptable for computing ventilation distributions. This method used by Wagner and co-workers computes the distribution of ventilation-perfusion ratios from a data curve relating the solubilities and the changes in arterial and expired air concentrations of several inert gasses artificially introduced into the bloodstream. The adapted algorithm computes ventilation distributions using data from an inert gas washout curve. Lewis and his colleagues (1978) have used a similar 50-compartment model to compute ventilation distributions from inert gas washout data and have used the results to identify ventilation distributions which correlate with certain lung diseases. A similar compartmental lung model is used in this investigation to compute ventilation distributions. Instead of using clinical data to compute the ventilation distribution curves the lung model developed by Calvert (1980) is used to provide the inert gas washout data. The 50-compartment model is not yet in use for computing the ventilation distribution due to some difficulties in adapting the least squares approach used to analyze the inert gas washout data.

LITERATURE CITED

- Burton, R.E., W.F. Storm, L.W. Johnson, S.D. Leverett, Jr. and B.O. Hartman. Stress Response of Pilots Flying High Performance Aircraft during Aerial Combat Maneuvers, Review of Air Force Sponsored Basic Research in Environmental and Acceleration Physiology, 1976. Wright-Patterson AFB, Ohio.
- Calvert, R.E. An Examination of the Effects of Acceleration Forces on Pulmonary Mechanics and Ventilation Using a Mathematical Simulator. PH.D. Dissertation. The University of Houston, 1980.
- Collins, R.E., R.W. Kilpper and D.E. Jenkins. A Mathematical Analysis of Mechanical Factors in the Forced Expiration. Bull. of Mathematical Biophysics. 29:737, 1967.
- Comroe, J.H., Jr., R.E. Forster, A.B. Dubois, W.A. Briscoe and E. Carlsen. The Lung, Year Book Medical Publishers, Inc., Chicago, 1962.
- Comroe, J.H., Jr. Physiology of Respiration, Year Book Medical Publishers, Inc., Chicago, 1974.
- Denison, D.M., N.J.H. Davies, M. Meyer, R.J. Pierce, and P. Scheid. Single Exhalation Method for Study of Lobar and Segmental Lung Function by Mass Spirometry in Man. Respir. Physiol. 42:87, 1980.
- Dolfuss, R.E., J. Milic-Emili, and D.V. Bates. Regional Ventilation of the Lung, Studies with Boluses of Xenon-133. Respir. Physiol. 2:234, 1967.
- Dollery, C.T., and P. Hugh-Jones. Distribution of Gas and Blood in the Lungs in Disease. Br. Med. Bull. 19:59, 1963.
- Gomez, D.M. A Physico-Mathematical Treatment of the Distribution of Specific Tidal Volume Throughout the Lung. Fed. Proc. 21:439, 1962.
- Gomez, D.M. A Mathematical Treatment of the Distribution of Tidal Volume Throughout the Lung. Proc. Nat. Acad. Sci. 49:312, 1963.
- Lewis, S.M., J.W. Evans, and A.A. Jalowayski. Continuous Distributions of Specific Ventilation Recovered from Inert Gas Washout. J. Appl. Physiol. 44:416-423, 1978.
- Rehder, K., A.D. Sessler and J.R. Rodarte. Regional Intrapulmonary Gas Distribution in Awake and Anesthetized-Paralyzed Man. J. Appl. Physiol. 42:391, 1977.
- Saidel, G.M., T.C. Militano and E.H. Chester. Pulmonary Gas Transport Characterization by a Dynamic Model. Resp. Physiol. 12:305, 1971.

Schmid, E.R., K. Rehder, T.J. Knopp, and R.E. Hyatt. Chest Wall Motion and Distribution of Inspired Gas in Anesthetized Supine Dogs. *J. Appl. Physiol.* 49:279, 1980.

Wagner, Peter D., Herbert A. Saltzman, and John B. West. Measurement of Continuous Distributions of Ventilation-Perfusion Ratios: Theory. *J. Appl. Physiol.* 36:588, 1974.

West, J.B. Ventilation-Perfusion Inequality and Overall Gas Exchange in Computer Models of the Lung. *Resp. Physiol.* 1:88, 1969.

END

FILMED

1-84

DTIC